Radiation Forces on Small Particles in the Solar System[1]

JOSEPH A. BURNS

Cornell University,[2] *Ithaca, New York 14853 and NASA-Ames Research Center*

PHILIPPE L. LAMY

CNRS–LAS, Marseille, France 13012

AND

STEVEN SOTER

Cornell University, Ithaca, New York 14853

We present a new and more accurate expression for the radiation pressure and Poynting–Robertson drag forces; it is more complete than previous ones, which considered only perfectly absorbing particles or artificial scattering laws. Using a simple heuristic derivation, the equation of motion for a particle of mass m and geometrical cross section A, moving with velocity v through a radiation field of energy flux density S, is found to be (to terms of order v/c)

$$m\dot{\mathbf{v}} = (SA/c)Q_{pr}[(1 - \dot{r}/c)\hat{\mathbf{S}} - \mathbf{v}/c],$$

where $\hat{\mathbf{S}}$ is a unit vector in the direction of the incident radiation, $\dot{r}$ is the particle's radial velocity, and c is the speed of light; the radiation pressure efficiency factor $Q_{pr} \equiv Q_{abs} + Q_{sca}(1 - \langle\cos \alpha\rangle)$, where Q_{abs} and Q_{sca} are the efficiency factors for absorption and scattering, and $\langle\cos \alpha\rangle$ accounts for the asymmetry of the scattered radiation. This result is confirmed by a new formal derivation applying special relativistic transformations for the incoming and outgoing energy and momentum as seen in the particle and solar frames of reference. Q_{pr} is evaluated from Mie theory for small spherical particles with measured optical properties, irradiated by the actual solar spectrum. Of the eight materials studied, only for iron, magnetite, and graphite grains does the radiation pressure force exceed gravity and then just for sizes around $0.1 \mu m$; very small particles are not easily blown out of the solar system nor are they rapidly dragged into the Sun by the Poynting–Robertson effect. The solar wind counterpart of the Poynting–Robertson drag may be effective, however, for these particles. The orbital consequences of these radiation forces—including ejection from the solar system by relatively small radiation pressures— and of the Poynting–Robertson drag are considered both for heliocentric and planetocentric orbiting particles. We discuss the coupling between the dynamics of particles and their sizes (which diminish due to sputtering and sublimation). A qualitative derivation is given for the differential Doppler effect, which occurs because the light received by an orbiting particle is slightly red-shifted by the solar rotation velocity when coming from the eastern hemisphere of the Sun but blue-shifted when from the western hemisphere; the ratio of this force to the Poynting–Robertson force is $(R_\odot/r)^2[(w_\odot/n) - 1]$, where $R_\odot$ and $w_\odot$ are the solar radius and spin rate, and n is the particle's mean motion. The Yarkovsky effect, caused by the asymmetry in the reradiated thermal emission of a rotating body, is also developed relying on new physical arguments. Throughout the paper, representative calculations use the physical and orbital properties of interplanetary dust, as known from various recent measurements.

---

[1] An invited review paper to *Icarus*.

[2] Current address.

I. INTRODUCTION

This article discusses the forces due to solar radiation incident on small particles: radiation pressure, Poynting–Robertson drag, the Yarkovsky effect, and the differential Doppler effect. The paper also considers the resulting orbital evolution for particles moving about the Sun and about planets, and to a lesser extent attempts to correlate theoretical results with dust observations, principally made by *in situ* measurements in space. While the subject has been studied for more than 70 years, the details of the relevant processes are not easily accessible from the literature. We have, therefore, rederived most results so as to clarify and generalize them. We have also carried out more complete numerical calculations of the coefficients that appear in the expressions. A recent brief review of some of these processes was done by Dohnanyi (1978).

Before describing the radiation forces that act on interplanetary dust, it will be valuable to outline the observational evidence for such particles and to list various review articles summarizing this information. Meteors, curved comet tails, and the zodiacal light are all indicators of interplanetary dust visible to the naked eye. Sporadic and shower meteors (see Soberman, 1971; Millman, 1976; Hughes, 1978) are observable when interplanetary meteoroids pass through the upper atmosphere; the survivors of this journey account for the extraterrestrial dust found in cores taken from the ocean floor and from polar ice. Such dust has even been captured by high-altitude aircraft (Brownlee *et al.*, 1977) and discovered in deep-sea sediments (Ganapathy *et al.*, 1978). Arcuate comet tails are composed of particles which escape the cometary nucleus and move on their own slightly different solar orbits due to nongravitational forces (cf. Beard, 1963; Finson and Probstein, 1968a, 1968b; Marsden, 1974; Vanysek, 1976; Whipple and Huebner, 1976; Whipple, 1978). The

zodiacal light (see Leinert, 1975; Weinberg and Sparrow, 1978), a faint glow in the night sky principally visible along the ecliptic, is due to the scattering of solar radiation by dust particles, which may derive from cometary or asteroidal detritus; as observed from Earth (Dumont, 1976) and by the photopolarimeters on Pioneers 10 and 11 (Weinberg, 1976), the zodiacal light intensity peaks near the Sun, decaying rapidly with ecliptic latitude and solar elongation except for a slight brightening in the antisolar direction, the gegenschein. The Pioneer and Helios spacecraft, as well as several earlier *in situ* observatories, have directly measured dust with impact counters of various types (Fechtig, 1976; Fechtig *et al.*, 1978; McDonnell, 1978). Nature itself has provided integral counters of a sort in the impacts recorded as surface microcraters found on otherwise smooth glass spheres on the lunar surface (Hörz *et al.*, 1971, 1975; Hartung 1976; Ashworth, 1978) and in some meteorites (Brownlee and Rajan, 1973). Not only is dust present in the solar system, but its existence in clouds throughout interstellar space is strongly implied by the extinction, reddening, and polarization of starlight (see Aannestad and Purcell, 1973; Huffman, 1977; Ney, 1977; Day, 1977; Greenberg, 1978). Dust can be produced in circumstellar space and can escape into interstellar space (cf. Dorschner, 1971). It may even lie in the intergalactic void (Margolis and Schramm, 1977). Although the number densities, composition, and origin of dust particles may be controversial, their existence is not.

The orbits of larger particles are also influenced by radiation forces. The impacts of such solar-orbiting particles are registered by lunar seismometers (Duennebier *et al.*, 1976); similar bodies impacting the Earth are found as meteorites (see Wetherill, 1974). Other evidence for interplanetary boulders (5–200 m) is indirect (Kresák, 1978). Dohnanyi (1972) summarizes information on the number density of all interplanetary masses.

The precise origin of the interplanetary particles causing the above phenomena is unclear (see Whipple, 1976). Certainly some interplanetary material in sizes less than a centimeter or so comes from comets, as attested to by Type II tails (Whipple, 1955, 1978; Vanysek, 1976; cf. Sekanina and Schuster, 1978a,b; Parthasarathy, 1979) and the correlation between meteor showers and cometary orbits. Dust must be generated as well in collisions between larger meteoroids (Dohnanyi, 1971; 1976b). Other interplanetary particles may be captured or transient interstellar grains (Best and Patterson, 1962; Radzievskii, 1967; Bertaux and Blamont, 1976; cf. Levy and Jokipii, 1976). Direct condensation in interplanetary space, or perhaps even in sunspots (Hemenway, 1976; cf. Mullan, 1977), might be a further source. Large particles—but still objects whose orbits are affected by radiation forces—probably derive from extinct cometary nuclei or represent the small end of the asteroidal size distribution. Notwithstanding these other possibilities, the current view is that most dust comes from cometary matter while large rocky particles are from the asteroids.

To select among the proposed origins for any sample of interplanetary dust (as retrieved from a balloon, spacecraft, or core sample), one must understand the dynamics of such particles and the evolution of their orbits. Such knowledge is valuable also in determining the size of the sources and sinks that govern the total mass of interplanetary matter and in interpreting the observational evidence. Finally, it is important in assessing the danger that spacecraft might incur in hitherto unexplored regions of the solar system (Millman, 1971).

In general the motion of small particles in space over short times is dominated by the preponderant gravitational presence of the Sun. However, the long-term evolution of such bodies is commonly produced by non-gravitational forces (radiation forces or collisions) because these change a body's total mechanical energy and angular momentum [see the orbital perturbation equations as developed by Burns (1976)]. In this review, we discuss, derive, and explain the forces that arise from interactions between small particles and solar radiation. The explanation of these radiation forces was a problem that attracted the notice of several eminent scientists around the turn of the century, notably Poynting, Larmor, and Plummer. It was even included briefly in Einstein's (1905) classic paper on special relativity. The correct expression for radiation pressure and Poynting–Robertson drag was the subject of some dispute at the time, as summarized by Robertson (1937) and Lyttleton (1976), who give pertinent historical references.

We first provide a simple heuristic derivation of the radiation pressure and Poynting–Robertson drag felt by a perfectly absorbing particle, as preparation for a new derivation of the complete expression which considers scattering as well as absorption. The results are confirmed by deriving them again in a more formal manner, using the transformation laws for energy and momentum from special relativity. Numerical values are presented and discussed for the forces experienced by small spherical particles composed of real materials that are irradiated by the actual solar spectrum; these demonstrate that radiation pressure and Poynting–Roberston drag in the solar system are significant only for particles in a rather narrow size range. In fact for very small particles ($\lesssim 10^{-2}$ μm) the corresponding drag due to solar corpuscular radiation is actually more important than that due to photons. The orbital consequences of the Poynting–Robertson drag and radiation pressure, including possible loss by orbital collapse or ejection, are also considered for heliocentric particles. The influence of these same forces on particles circling planets is discussed. In addition we outline the coupling between the dynamics of particles and their sizes (which shrink with time owing to sublimation and sputtering). A short qualitative description is given

for the Yarkovsky effect, which is important for particles in the meter-to-kilometer range, particularly for those made of stony materials. Also briefly mentioned is a new effect, the differential Doppler effect, discovered by McDonough (1975), which may be appreciable in other planetary systems.

Although certainly important for particles of special size and composition, the direct interaction with the interplanetary electromagnetic field of the solar wind will not be discussed because to date an accurate treatment of the electric potential of interplanetary objects is not available (Belton, 1966), although recent progress has been made (see papers in Grard, 1973); also the dynamics for a particle with a given electric charge are not well developed (cf. Parker, 1964; papers in Weinberg, 1967; Standeford, 1968; Lamy, 1975; Levy and Jokipii, 1976) but advances (Consolmagno and Jokipii, 1977; Consolmagno, 1978) are occurring. It seems possible that such forces are responsible for the north–south asymmetry seen in the zodiacal light cloud of the inner solar system by Helios (C. Leinert, personal communication, 1976). We review here only those forces that involve the momentum carried by radiation, and so neglect such effects as, for example, those due to the stochastic collisions between orbiting particles (see Whipple, 1955; Kresák, 1976) or the nonuniform evaporation of rotating comet nuclei (Marsden, 1974). We also do not account for the influence of any gravitational force other than that due to a point mass primary (i.e., quadrupole terms and planetary perturbations are ignored; see Misconi and Weinberg, 1978).

II. RADIATION PRESSURE AND POYNTING–ROBERTSON DRAG

Bodies in interplanetary space are not only attracted to the Sun by gravity but are also repelled from it by radiation pressure due to the momentum carried in solar photons. The orbits of such particles are also modified by the velocity-dependent Poynting–Robertson effect, the nature of

which has been the subject of considerable controversy and misunderstanding since the beginning of the century, receiving its fundamentally correct—although incomplete and abstruse—treatment by Robertson (1937).

Unfortunately, Robertson's derivation was unnecessarily difficult because it relied on the metric of special relativity even though, as shown below, the result can be derived and understood in classical terms without invoking space-time dilatation. Furthermore, Robertson's expression explicitly contained an important assumption which is usually overlooked: he considered only perfectly absorbing particles whereas, in general, small particles scatter or transmit most of the energy incident on them. This deficiency in Robertson's expression was noted by Mukai et al. (1974) and Lamy (1976a), who (incorrectly) considered the drag to be caused by the absorbed energy only; we shall see below that the scattered energy is just as important. To our knowledge, a general expression for this term has not previously been included correctly, although Lyttleton (1976) derived the forces for a specific, but artificial, scattering law. Hämeen-Anttila (1962) instead erred by merely multiplying the radiation force by a constant.

Perhaps it is in part due to Robertson's abstruse derivation and in part to the subsequent neglect of scattering that most textbook explanations of the Poynting–Robertson effect have been confusing and/or inaccurate. Even though the effect is essential to an understanding of the orbital evolution of small interplanetary (and circumplanetary) particles, we are not aware of any simple but accurate and complete derivation except for our prior developments (Soter et al., 1977; Burns and Soter, 1979), from which the complete absorption case of the derivation below closely follows, although the approaches of Best and Patterson (1962) and Harwit (1973, p. 176) are somewhat similar to it.

In order to clarify the problem, we present two derivations, one heuristic and the

other formal. The heuristic derivation is approached in two stages, first considering only perfectly absorbing particles in order to obtain Robertson's expression (but on a much simpler physical basis), and then applying an even more elementary model of colliding particles to find the correct general expression for a particle that scatters, transmits, and absorbs light. These results will be supported by rederiving them in a more rigorous and methodical manner using transformation laws from special relativity. After developing and discussing the correct expressions, we provide numerical values of the solar radiation forces felt by small particles of cosmochemically important compositions.

III. HEURISTIC DERIVATION OF RADIATION FORCES

Perfectly Absorbing Particles

The force on a perfectly absorbing particle due to solar (photon) radiation can be viewed as composed of two parts: (a) a *radiation pressure* term, which is due to the initial interception by the particle of the incident momentum in the beam, and (b) a *mass-loading drag,* which is due to the effective rate of mass loss from the moving particle as it continuously reradiates the incident energy.

The total amount of energy intercepted per second from a radiation beam of integrated flux density S(ergs $cm^{-2}sec^{-1}$) by a stationary, perfectly absorbing particle of geometrical cross section A is SA. If the particle is moving relative to the Sun with velocity v, we must replace S by

$$S' = S(1 - \dot{r}/c), \qquad (1)$$

where $\dot{r} = v \cdot \hat{S}$ is the radial velocity (Fig. 1), $\hat{S}$ is a unit vector in the direction of the incident beam, and c is the speed of light; the factor in parentheses is due to the Doppler effect, which alters the incident energy flux by shifting the received wavelengths. The momentum removed per second from the incident beam as seen by the particle is then $(S'A/c)\hat{S}$. This is the *radiation pressure*

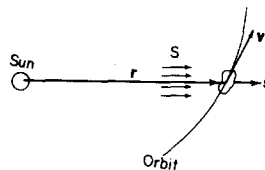FIG. 1. A schematic diagram illustrating an orbiting particle being struck by solar radiation of flux density S ergs cm^{-2} sec^{-1}. The particle is of mass m and cross section A; it is located at r and is moving with velocity v. The unit vector parallel to the radiation beam is $\hat{S}$.

force, as can be understood by recalling Newton's second law: a time rate of change of linear momentum requires an impressed force.

The absorbed energy flux $S'A$ is continuously reradiated from the particle. Since the reradiation is nearly isotropic (small particles being effectively isothermal), there is no net force exerted thereby on the particle in its own frame. However, the reradiation is *equivalent* to a mass loss rate of $S'A/c^2$ from the moving particle—which has velocity v as seen from the inertial frame of the Sun—and, as measured in the solar frame, this gives rise to a momentum flux from the particle of $-(S'A/c^2)v$, schematically shown in Fig. 2. Since the particle is losing
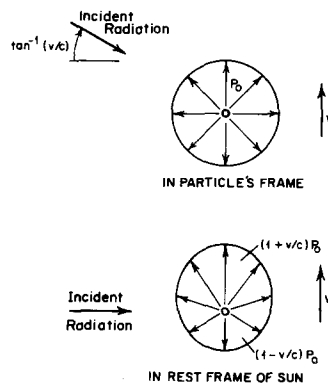

FIG. 2. A schematic illustration that reradiation preferentially emits $S'Av/c^2$ more momentum in the forward direction, as seen from the solar frame of reference, because the frequencies (and momenta p) of the quanta reradiated (or scattered) in the forward direction are increased over those in the backward direction. The length of the vectors in the reemitted radiation pattern show the momenta in the two frames of reference.

momentum while its mass is in fact always conserved, the particle is decelerated: it suffers a dynamical drag. The momentum loss per unit time represents, according to the impulse–momentum theorem, a force on the particle of the same amount; this is sometimes called the *Poynting–Robertson drag*.

The net force on the particle is then the sum of the forces due to the impulse exerted by the incident beam and the momentum density loss from the moving particle or, for a particle of mass m,

$$m\dot{v} = (S'A/c)\hat{S} - (S'A/c^2)v$$
$$\cong (SA/c)[(1 - \dot{r}/c)\hat{S} - v/c], \quad (2)$$

to terms of order v/c. This last expression is equivalent to Robertson's (1937) result.

Scattering Particles

In general, as Fig. 3 illustrates, a small (spherical) particle of geometrical cross section A will scatter an amount of light equivalent to that incident on an area AQ_{sca}, and absorb that incident on AQ_{abs}, where Q_{sca} and Q_{abs} are defined as the scattering and absorption coefficients, respectively; that is, they correspond to the fractional amounts of energy scattered and absorbed. For a given particle, Q_{sca}, Q_{abs}, and Q_{pr} (to be defined) depend on wavelength; in the derivations that follow, we take them to be average values, computed by integrating
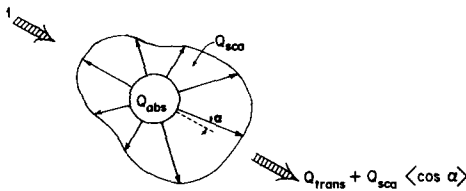

FIG. 3. An illustration of the efficiency factors of optics. One unit of energy is seen entering the upper left-hand edge: Q_{abs} is absorbed by the particle, Q_{sca} is scattered in a pattern that is symmetric about the radiation beam while Q_{trans} is transmitted. In the scattered beam a momentum of Q_{sca} $\langle\cos \alpha\rangle$ is sent in the forward direction, where $\langle\cos \alpha\rangle$ is the asymmetry factor, i.e., the weighted average of the angular dependence of the scattered radiation. $Q_{abs} + Q_{sca} + Q_{trans} = 1$, ignoring diffraction.

over the actual solar spectrum. These coefficients will be calculated later from Mie theory.

The scattering diagram resulting from unpolarized light incident on a spherical particle has rotational symmetry about the radial direction $\hat{S}$. The intensity of the scattered light thus depends only on the angle α it makes with the incident beam direction (where $\alpha = 0$ corresponds to forward-scattering). The energy scattered into the incremental solid angle annulus $d\chi = 2\pi \sin\alpha \, d\alpha$ in the direction α is proportional to $f(\alpha)d\chi$, where $f(\alpha)$ is the phase function of the scattering particle, normalized so that $f(\alpha)d\chi$ integrated over all directions is unity. Then the net energy flux anisotropically scattered per second into the *forward* direction is $S'AQ_{sca}\langle\cos \alpha\rangle\hat{S}$, where the anisotropy parameter,

$$\langle\cos \alpha\rangle \equiv \int_{4\pi} f(\alpha) \cos \alpha \, d\chi, \quad (3)$$

can be calculated, again from Mie theory. When the scattering on the average is in the direction of the beam, $\langle\cos \alpha\rangle$ is a positive number whereas it is negative for reflected radiation.

The radiation pressure coefficient,

$$Q_{pr} \equiv Q_{abs} + Q_{sca}(1 - \langle\cos \alpha\rangle), \quad (4)$$

will appear in the expressions for the forces felt by particles having general optical properties. For a stationary particle (at least) this factor multiplies the incident momentum flux to transform it into the radiation pressure force. In perfect forward-scattering, $Q_{pr} = Q_{abs}$; with isotropic scattering, $Q_{pr} = Q_{abs} + Q_{sca}$; while for perfect back-scattering, $Q_{pr} = Q_{abs} + 2Q_{sca}$. With more general scattering laws one can consider a portion of Q_{sca} to be scattered isotropically while the remainder has $\langle\cos \alpha\rangle = \pm 1$.

In order to compute the radiation forces felt by particles which both scatter and absorb radiation, we consider a simple model which involves colliding particles and mass exchange; these processes each cause

momentum transfer. This model contains the two features that were found to be important in the perfect absorption case: a pressure along the incident beam's direction and a drag, due to mass loading, along the particle's velocity. At the top of Fig. 4 a particle of mass m, moving with velocity v, is about to be struck by a beam of projectiles, M per second, which travel relative to the stationary frame with velocity c, not necessarily the speed of light. In the middle panel the same scene is viewed one second after the first projectile in the stream strikes m. In the meantime $M' = M(1 - v \cos \xi/c)$ mass has collided with m; a fraction fM' of this has been absorbed but is continuously reemitted (or, equivalently, isotropically scattered) so as to keep the particle's mass m constant. The remaining mass gM' which strikes the particle leaves it with the same relative vector velocity with which it arrived; to mimic the two cases of interest for radiation, this means that, if forward-scattered, gM' passes directly through m while, if backscattered, it undergoes perfect reflection (see Fig. 4c). Based on our experience with totally absorbing particles, we permit the particle's velocity to be modified following the interaction with the beam in two ways: ΔV per second in the direction of the beam's original momentum is the acceleration due to the radiation pressure whereas Δv per second along particle's velocity vector is the deceleration due to mass loading. Although these two components are not orthogonal, obviously they give a complete description of the particle's response since this is a two-dimensional problem.

Conservation of linear momentum in the x and y directions will provide Δv and ΔV. For this we consider that fM' still resides in m, as shown in Fig. 4b, since it has no momentum relative to the particle while its momentum density seen in the stationary frame is identical to the particle's. Equating the momentum in the y direction before and after the interaction, we have

$$mv \sin \xi = (m + fM')(v + \Delta v) \sin \xi \\ + gM'[(\mp)v \sin \xi + v \sin \xi],$$

where here, and throughout this section, the top sign corresponds to forward-scattering and the bottom sign to back-scattering. The first part of the bracketed term is then the vertical velocity of the scattered beam as measured relative to the particle; in magnitude, it is the y component of the received velocity according to the particle. The last part of this term accounts for the fact that the previous measurement is accomplished relative to a moving frame whose velocity is $v \sin \xi$; we ignore any change in v during the interaction. Realizing that $f + g = 1$ and assuming that $\Delta v \ll v, c$ and that $M \ll m$, we find that

$$\Delta v = -(1 \mp g)M'v/m;$$

this slowing of the particle along its path we interpret as being caused by a mass-loading drag.

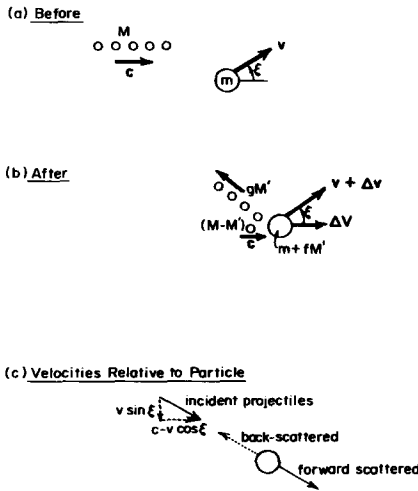We can now determine ΔV in the same

FIG. 4. A nonrelativistic model to demonstrate radiation pressure and Poynting–Robertson drag. (a) The top diagram shows a beam of projectiles on its way to strike a particle. (b) A fraction fM' of the projectiles has been absorbed and then isotropically reemitted (or isotropically scattered). The remainder gM' is either forward-scattered or back-scattered; here it is shown back-scattered. (c) The interaction as viewed from the particle where only the incident and the scattered radiation are seen.

way from conservation of the x momentum

$$Mc + mv \cos \xi$$
$$= (m + fM')[(v + \Delta v) \cos \xi + \Delta V]$$
$$+ gM'[\pm(c - v \cos \xi) + v \cos \xi]$$
$$+ (M - M')c.$$

The last term represents the momentum in the beam which has not collided with the particle because of the latter's motion. The penultimate term assumes once again that the projectiles leave with the identical relative velocity they had on approach. Using the same approximations as for the drag case and substituting for Δv, we arrive at

$$\Delta V = (1 \mp g)M'c/m;$$

this is produced by the momentum in the beam. It is the radiation pressure in the case where the impacting beam is composed of photons.

The total effect of the projectile beam can be found by vectorially adding the two velocity changes

$$\Delta V + \Delta v = (1 \mp g)(M'/m)(c\hat{S} - v);$$

in actuality this is an acceleration since it occurs every second.

The transference of this result from colliding material objects to the case when radiation instead strikes a particle is direct, since we can associate $\mp g$ with $-Q_{sca}\langle \cos \alpha \rangle$ and $f + g = 1$ with $Q_{abs} + Q_{sca}$; we note however that, owing to diffraction, $Q_{abs} + Q_{sca}$ need not be unity for microscopic particles. Any directly transmitted radiation is the same as scattered radiation with $\langle \cos \alpha \rangle = 1$. Therefore from (4) we have that

$$\mathbf{F}_{rad} = m\dot{\mathbf{v}} = Q_{pr}M'(\mathbf{c} - \mathbf{v}),$$

where M' is the "mass" of the photons which strike the particle or $(S'A/c^2)$. In the above form, the radiation force can be viewed as a drag force caused by the relative velocity, $\mathbf{c} - \mathbf{v}$, of the particle through a beam of photons. Finally, to terms of order v/c, we can write the net force on the particle as

$$m\dot{\mathbf{v}} \cong (SA/c)Q_{pr}[(1 - \dot{r}/c)\hat{S} - \mathbf{v}/c]. \quad (5)$$

For a totally absorbing particle this reduces to (2) since then $Q_{pr} = 1$. Equation (5) is identical to Robertson's expression except for being more general by the inclusion of the important factor Q_{pr}. We note, however, from the above derivation that radiation forces—including the Poynting–Robertson drag—are *fundamentally classical* forces and are not produced by relativistic effects as commonly believed.

For *heliocentric* particles with $\mathbf{v} = \dot{r}\hat{r} + r\dot{\theta}\hat{\theta}$, where $\hat{r} = \hat{S}$ is the orbital radius unit vector and $\hat{\theta}$ is normal to $\hat{r}$ in the orbit plane, we can also write the radiation force as

$$m\dot{\mathbf{v}} \cong (SA/c)Q_{pr}[(1 - 2\dot{r}/c)\hat{r} - (r\dot{\theta}/c)\hat{\theta}]. \quad (6)$$

Usually we call the velocity dependent portion of (6) the *Poynting–Robertson drag* and the constant radial term the *radiation pressure;* others say that the radial factor in this expression is the radiation pressure while the transverse term is the Poynting–Robertson drag; still others call the coefficient of the $\hat{S}$ term in (5) the radiation pressure and the term proportional to $\mathbf{v}$, the Poynting–Robertson drag.

To gain familiarity with the radiation forces, we consider the right-hand side of the equation of motion (6) in some limiting cases. These "tests" amount to understanding the meaning of Q_{pr} as given by (4). *Perfect transmission*—that is, no particle—occurs when $Q_{pr} = 0$. *Complete absorption,* the case considered by Robertson (1937), has $Q_{pr} = Q_{abs} = 1$, even including diffraction since the diffracted light has zero contribution (van de Hulst, 1957, p. 225), and so our results agree with the classical ones. Any *forward-scattered* radiation ($\langle \cos \alpha \rangle = 1$) produces neither radiation pressure, nor a drag, because the beam just passes through the body, continuing radially outwards from the Sun as though there had been no particle. An *isotropically scattering* particle, such as a *perfect reflector,* has $Q_{pr} = Q_{abs} + Q_{sca}$. A particle which *perfectly backscatters* undergoes

twice the drag of a totally absorbing or a perfectly reflecting particle. This happens because electromagnetic momentum is carried by the back-scattered beam in the direction of the particle's motion since its component in that direction is due to the angle $(2v/c)$ of reflection; this momentum is withdrawn from the particle's motion. A *stationary particle* feels a radiation pressure without a Doppler shift and, of course, has no Poynting–Robertson drag.

Mass Loss and the Principle of Relativity

The forces we have derived presume the particle's mass to be constant; it remains the same even though the body is continually radiating energy (and therefore mass) because the body absorbs just as much energy. (It is, by definition, in thermal equilibrium.) If we consider a particle that is *not* in thermal equilibrium and which is radiating into free space, its mass decreases. The loss of mass occurs at precisely the correct rate so that, considering the momentum loss, the particle velocity stays constant, permitting the principle of relativity to be satisfied. Whether relativity would hold was a matter of considerable dispute in the early part of the century when Larmor and Poynting each had written incorrect coefficients on the drag term, meaning that they produced results which violated relativity (cf. Robertson, 1937).

Note that, for any particle in thermal equilibrium, the energy radiated away carries with it mass and linear momentum in exactly the ratio needed to conserve the particle's linear momentum density (i.e., velocity). On the other hand, the absorbed radiation brings in only mass and not a concomitant increase in transverse momentum. This added mass burdens the particle so that it slows down. We emphasize that the Poynting–Robertson drag takes place because the momentum in the incoming and outgoing radiation is not the same: any such body in thermal equilibrium will suffer a decelerating drag. The drag does not result from the directed character of the solar

beam itself but rather from the momentum exchange process.

IV. FORMAL CALCULATION OF RADIATION FORCES USING SPECIAL RELATIVITY TRANSFORMATIONS

In order to lend credence to the above expressions for the radiation pressure force and Poynting–Robertson drag, we derive the same results here in a more rigorous manner. We do this in order to end once and for all the controversy over the correct coefficients for these expressions. However, a reader who feels comfortable with the previous derivations and who is not interested in the fine points of a formal demonstration is advised to skip over this section.

To find the forces experienced by a particle of constant mass moving through a beam of radiation, we use the principle of conservation of total linear momentum, including electromagnetic in addition to mechanical momentum. We take into account the various interactions the particle has with the radiation as seen in both the solar and particle frames of reference. In this way we can calculate the electromagnetic momentum added per unit time to the beam; this must equal the mechanical momentum lost per unit time by the particle. By the impulse-momentum theorem, the latter quantity is the force acting on the particle. This very direct, although cumbersome, approach does not appear to have been previously used to derive the Poynting–Robertson force, with one notable exception: Einstein (1905) computed the radiation pressure on a moving perfect reflector in a way very similar to ours and stated, "All problems in the optics of moving bodies can be solved by the method here employed." We humbly agree.

The following transformation law (Jackson, 1962, p. 392) for the four-vector of momentum-energy is used throughout:

$$
\begin{aligned}
p_x &= p_{x'}, \\
p_y &= p_{y'}, \\
p_z &= \gamma[p_{z'} + (v/c)(E'/c)], \\
p_4 &\equiv iE/c = i\gamma(E' + vp_{z'})/c,
\end{aligned}
\qquad (7)
$$

where $\gamma \equiv (1 - v^2/c^2)^{-1/2}$ and $i \equiv \sqrt{-1}$; the primed quantities are measured in a frame of reference which moves with a velocity v along the positive z axis (to be specified). The same transformation can be applied to find quantities in the primed system in terms of unprimed values by merely interchanging primed and unprimed variables, and changing the sign of v.

Since the particle velocities relative to the Sun are small in comparison to the speed of light c, we will consider two separate cases—the particle moving with a purely transverse velocity v relative to the beam and then having purely radial motion u—and merely add the results from them together.

Transverse Motion

The case of purely transverse motion corresponds to a particle on a perfectly circular orbit, ignoring the centrifugal acceleration. The situation is shown in Fig. 5, where the solar frame is centered on the Sun and the other frame is attached to the particle which moves with uniform velocity v in the z (tangential) direction.

As seen by a solar observer when a radiation beam of energy flux E_i strikes the particle, the incoming four-vector of momentum-energy flux contained in it is

$$\mathbf{p}_i = (p_x, p_y, p_z, iE/c)$$
$$= (-E_i/c, 0, 0, iE_i/c), \quad (8)$$

where the first three components of the row vector are the x, y, z momentum fluxes while the fourth is the energy flux in momentum units. According to an observer on the particle, this vector is
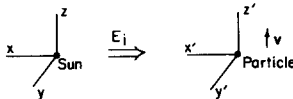

FIG. 5. The frame of reference attached to the particle moves with transverse velocity v in the z(z') direction relative to the frame of reference attached to the Sun. E_i is the energy per second striking the particle as seen by an observer on the Sun.

$$\mathbf{p}_i' = (p_{x'}, p_{y'}, p_{z'}, iE'/c)$$
$$= (-E_i/c, 0, -\gamma E_i v/c^2, i\gamma E_i/c) \quad (9)$$

by a direct application of the transformation law (7). We note that the beam's trajectory makes an angle with respect to the x axis of $\psi = \tan^{-1}(p_z/p_x) = \gamma v/c$ as seen by the particle; this agrees with the transformation law for angles (Jackson, 1962, p. 362). This then is the radiation which strikes the particle: some is scattered, some is absorbed to be immediately reemitted isotropically, and the rest passes directly through. All these interactions can be described by the same optical cross sections defined earlier (and to be calculated in Section VI), since the particle is stationary in *this* reference frame. After inserting these cross sections, one finds that the outgoing radiation leaving the vicinity of the particle has a four-vector momentum flux of

$$\mathbf{p}_0' = [-(E_i/c)(1 - Q_{pr}), 0,$$
$$-(\gamma E_i v/c^2)(1 - Q_{pr}), i\gamma E_i/c], \quad (10)$$

as seen by an observer in the particle's frame of reference. Equation (7) permits this to be transformed at once to the outgoing momentum flux as seen in the solar frame,

$$\mathbf{p}_0 = [-(E_i/c)(1 - Q_{pr}),$$
$$0, (\gamma^2 E_i v/c^2)Q_{pr},$$
$$i(1 + \gamma^2 Q_{pr} v^2/c^2)E_i/c]. \quad (11)$$

Equations (8) and (11) express the interaction of the radiation beam with the particle as seen from a specific frame of reference. Since the system is isolated, any change in the electromagnetic momentum flux must be directly associated with a change of opposite sign in the particle's mechanical momentum flux. But the change per unit time in the linear mechanical momentum of the particle is, by Newton's second law, equal to a force. The force felt by a transversely moving particle, then, is minus the four-vector momentum loss per unit time from the beam, or

$$\mathbf{F}_v = -\Delta \mathbf{p} = \mathbf{p}_i - \mathbf{p}_0$$
$$= [-Q_{pr}E_i/c, 0, \ -(Q_{pr}E_i/c)(\gamma^2 v/c),$$
$$-iQ_{pr}E_i\gamma^2 v^2/c^3] \quad (12)$$

in which $E_i = SA$.

The x term, since it is radial, is the radiation pressure force while the z term is the tangential Poynting–Robertson drag. Equation (12) agrees with our previous result (5) with the substitution $E_i = SA$ and $\dot{r} = 0$. Although it might appear that energy is not conserved because of the beam's energy gain expressed by minus the fourth component of (12), this added energy is lost from the particle's kinetic energy: $\Delta E_{beam} = \mathbf{F} \cdot \mathbf{v} = F_z v$. Note that the usual "explanation" of the Poynting–Robertson force as being the transverse component of the radiation pressure force, caused by the aberration of sunlight through an angle (v/c) as seen by the particle, is correct in the limit $v \ll c$, as is apparent by a comparison of the first and third components of (12).

Parallel Motion

We now consider the particle to be moving with velocity u in the direction of the radiation beam, i.e., radially as shown in Fig. 6. An identical approach to that used above for transverse motion is applied and similar expressions written for the incoming four-vectors of momentum-energy flux,

$$\mathbf{p}_i = [0, 0, E_i/c, iE_i/c],$$
$$\mathbf{p}_i' = \{0, 0, (E_i/c)[(1 - u/c)/(1 + u/c)]^{1/2},$$
$$(iE_i/c)[(1 - u/c)/(1 + u/c)]^{1/2}\}, \quad (13)$$

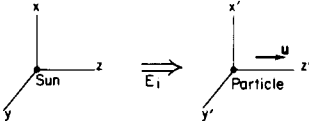and for the outgoing four-vectors of momentum-energy flux

FIG. 6. The frame of reference attached to the particle moves with radial velocity **u** in the $z(z')$ direction relative to the frame of reference attached to the Sun. E_i is the energy per second striking the particle as seen by an observer on the Sun.

$$\mathbf{p}_0' = \{0, 0, (E_i/c)(1 - Q_{pr})$$
$$[(1 - u/c)^{1/2}/(1 + u/c)^{1/2}],$$
$$(iE_i/c)[(1 - u/c)^{1/2}/(1 + u/c)^{1/2}]\},$$
$$\mathbf{p}_0 = \{0, 0, (E_i/c)$$
$$[1 - Q_{pr}/(1 + u/c)],$$
$$(iE_i/c)[1 - Q_{pr}u/c(1 + u/c)]\}. \quad (14)$$

The force experienced by a particle moving in the direction of the radiation beam is minus the four-vector momentum-energy flux loss from the beam

$$\mathbf{F}_u = -\Delta p$$
$$= [0, 0, (E_i/c)Q_{pr}/(1 + u/c),$$
$$(iE_i/c)Q_{pr}(u/c)[1/(1 + u/c)]. \quad (15)$$

The z term now includes a change in the radiation pressure force because of the motion. Once again the fourth term $-\Delta E_{beam} = \mathbf{F} \cdot \mathbf{u} = F_z u$ and so total energy is conserved. For $u \ll c$, the denominator of (12) can be accurately expanded to give

$$F_u = [0, 0, (SA/c)Q_{pr}(1 - 2u/c),$$
$$(iSA/c)Q_{pr}(u/c)(1 - 2u/c)] \quad (16)$$

in accord with result (6), substituting $\dot{r} = u$ and $\dot{\theta} = 0$ along with $E_i = SA(1 - u/c)$. The z component of (16) is the radiation pressure force as modified by a double Doppler shift; as seen from the heuristic derivation, one (u/c) comes from the rate at which energy is received, the other results from both the reradiated and scattered energy containing momentum.

As long as both u and $v \ll c$ (which is easily satisfied in solar system cases), we can linearly add the two force expressions (12) and (16) to find the total effect of the radiation on an arbitrarily moving particle. Using $\dot{r} = u$, and $r\dot{\theta} = v$, the final equation of motion is

$$\dot{\mathbf{v}} = (SA/mc)Q_{pr}[(1 - 2\dot{r}/c)\hat{\mathbf{r}}$$
$$- (r\dot{\theta}/c)\hat{\theta}], \quad (17)$$

which is, of course, identical to the previous result (6) and to Robertson's (1937) result when $Q_{pr} = 1$.

V. SOLAR WIND CORPUSCULAR FORCES

The conservation of momentum and energy approach that we have applied above is also useful in considering the forces produced by the solar wind, the particulate radiation from the Sun (cf. Whipple, 1955, 1967; Donnison and Williams, 1977b). Since the energy-momentum relation for nonrelativistic particles, $p = 2E/v_{sw}$ (where v_{sw} is the solar wind velocity), differs from that for electromagnetic radiation, we must appropriately change the energy terms that appear in the momentum portion of (12). The momentum and energy flux densities carried by the solar wind are on the average only 2×10^{-4} and 2×10^{-7}, respectively, of the amounts carried in the electromagnetic radiation; hence, since the corpuscular force is proportional to the momentum flux density, the total radiation pressure is little affected by solar wind particles striking the dust grain, even including its increased Coulomb cross section. Nevertheless, the counterpart of the Poynting–Robertson drag caused by solar wind particles can be significant because the aberration angle of the solar wind, $\tan^{-1}(v/v_{sw})$, is much larger than for the classical radiation case. The ratio of the two effects is

(corpuscular drag/radiation drag)

$$= (p_{sw}/p_{rad})(c/v_{sw})(C_D/Q_{pr}), \quad (17*)$$

where C_D is the drag coefficient. This ratio will be considered in more detail in the section on the dynamical consequences of Poynting–Robertson drag. In the next section we will find that Q_{pr} is small for metallic particles less than about 0.003 μm in radius and for particles of other materials less than 0.03 μm. This means that, in the present solar wind, such small particles will be eliminated by the pseudo-Poynting–Robertson drag of corpuscular radiation. At other times, or about other stars, corpuscular radiation pressure and drag may be even more significant.

VI. EVALUATION OF RADIATION PRESSURE EFFICIENCY FACTORS

Size and Shape of Interplanetary Dust

All that remains in order to find the radiation pressure and Poynting–Robertson drag forces actually experienced by small particles in interplanetary space is to evaluate the coefficient Q_{pr}. For this calculation, the particles are assumed to be spheres. While this is obviously done for reasons of computational simplicity, it has some observational justification. The shapes of lunar microcraters, and those found on returned spacecraft detectors, are often nearly circular, which, according to calibration experiments (Vedder and Mandeville, 1974; Fechtig et al., 1978), means that the impacting particles are approximately spherical (Brownlee et al., 1973; Hörz et al., 1975). To be more precise, if the particles are spheroids, typically their axes are in ratios less than 2:1. Furthermore U-2 aircraft, balloon, and rocket flights through the stratosphere and above it have retrieved numerous micrometeorites which are roughly equidimensional and are rarely of elongated or plate-like form. More often these interplanetary particles are irregular agglomerates built out of approximately spheroidal submicron elements (Brownlee et al., 1975, 1976, 1977; Brownlee, 1978a,b); the closest terrestrial analogs, perhaps, would be clusters of grapes or sacks of fish eggs. The structures are quite compact, with empty space comprising much less than half the volume, and typically have densities of 2 to 2.5 g cm^{-3}; this is in fair agreement with the derived density of 2 to 4 g cm^{-3} for the impacting bodies that cause the lunar microcraters but is in direct contradiction to the traditional view of "fluffy" meteoroids (cf. Giese et al., 1978). Space does contain some of the latter nonetheless, as evidenced by a fraction of the stratospheric micrometeorites being quite porous: $\rho \sim 1$ g cm^{-3} (Brownlee, 1978a,b). Most of the particles collected by

the U-2 aircraft are opaque, black aggregates (4–25 μm) built out of ~1000-Å size grains, which themselves are built up out of yet smaller grains less than ~100 Å in size. The cumulative elemental composition is chondritic (Brownlee, 1978a). Extraterrestrial vuggy spherules tens of microns in size have been found in deep-sea sediments; Parkin et al. (1977) propose that their shape may be intrinsic and not result from heating on passage through the terrestrial atmosphere. Theoretical support for the choice of spherical shapes also exists: recent analog studies, along with numerical modeling, show that a randomly oriented sample of irregular particles has, in the mean, much the same optical response as a sphere. The irregular particles are somewhat more efficient scatterers per unit mass due to their large surface area and they are more isotropic, with less forward-scattering and less back-scattering (Zerull, 1976; Zerull et al., 1977a; cf. Cuzzi and Pollack, 1978). However, as can be seen from any scattering diagram, the radiation pressure felt by the two classes of particles differs by significantly less than a factor of two in almost all cases.

Some comment is due here on the characteristic sizes of particles found in interplanetary space. Lunar microcrater studies show a monotonically increasing flux of particles throughout the size range from 1 mm to 10^{-2} μm; the crater counts for these sizes imply cratering fluxes of 10^{-5} to 10^{3} cm^{-2} year^{-1}sr^{-1}, respectively (Hörz et al., 1975; Morrison and Zinner, 1977; Le Sergeant and Lamy, 1979). A dip in the curve is seen somewhere around a few microns which, as discussed later, may be due to selective removal of particles about this size by either radiation pressure or Poynting–Robertson drag (see, however, Chernyak, 1978). Several hundred extraterrestrial particles have been captured in the Earth's upper atmosphere. The technique is successful for a limited range of sizes because contamination by terrestrial materials is a serious problem for particles less than a few microns and because particles larger than tens of microns are severely heated during entry (Brownlee, 1978b; Brownlee et al., 1977). Size distributions within this range have not been published but the total number density in the upper atmosphere is consistent with the interplanetary flux. Zodiacal light studies suggest to some (e.g., Giese and Grün, 1976; Leinert et al., 1976) that the scattering particles are "large" (~25 μm) but fluffy or irregular (Zerull et al., 1977b; Giese, 1977; Giese et al., 1978), whereas others (e.g., Dumont, 1976; Lillie, 1976) believe that substantial numbers of submicron particles are required to explain the polarization and ultraviolet results in addition to the north–south asymmetry of the zodiacal cloud. Micrometeoroid detectors aboard spacecraft are sensitive to particles in the 0.1- to 10-μm range (Fechtig, 1976; Fechtig et al., 1978); they have been most successful in determining the interplanetary and circumterrestrial number densities as functions of heliocentric distances and in identifying the orbital characteristics of the dust. Particles measured by these techniques are those for which radiation pressure and Poynting–Robertson drag are most significant. Meteor studies (Soberman, 1971; Millman, 1976; Hughes, 1978) give information on objects of centimeter size in the vicinity of the Earth. Information on yet larger objects, those for which the Yarkovsky effect will be most important, comes by extrapolating the meteor data up, or the asteroid data down, in size (Dohnanyi, 1972; 1976b; Ashworth, 1978); a useful review on the possible mass distribution of interplanetary boulders is by Kresák (1978).

Contrary to some early impressions (Hörz et al., 1975), measurements now indicate that the interplanetary dust flux has remained constant over the past 10^{6} years or so (Morrison and Zinner, 1977).

Definition of β

The gravitational attraction of the Sun

(mass M at distance r) upon a spherical particle of radius s and density ρ is

$$F_g = \tfrac{4}{3}\,\pi s^3 \rho GM/r^2, \qquad (18)$$

where G is the gravitational constant. The radiation pressure force due to solar radiation, as given in (5), is

$$F_r = (SA/c)Q_{pr},$$

using $S = L/4\pi r^2$ for the radiation flux density at distance r; L is the solar luminosity. We can also write $S = S_0(r_0/r)^2$, where $S_0 = 1.36 \times 10^6$ ergs cm^{-2} sec^{-1} is the solar constant and $r_0 = 1$ AU in centimeters. We then compare the radiation force to the gravitational force, defining their ratio by the parameter

$$\begin{aligned}\beta \equiv F_r/F_g &= (3L/16\pi GMc)(Q_{pr}/\rho s)\\ &= 5.7 \times 10^{-5}Q_{pr}/\rho s, \qquad (19)\end{aligned}$$

where Q_{pr} is averaged over the solar spectrum, and ρ and s are in cgs units. We have assumed that the Sun is a point source of radiation; for coronal particles this is not a good approximation and instead the solid angle Ω subtended by the Sun should be taken as $(\Omega/2\pi) = 1 - [1 - (R_\odot/r)^2]^{1/2}$ (Over, 1958) and, to be even more correct, the radiation pressure and Poynting–Robertson forces can be rederived (Guess, 1962). Limb darkening should also be included (Lamy, in preparation).

We see that the force ratio is independent of the distance from the Sun and thus the orbits remain conic sections even with the addition of radiation pressure. We note that β/Q_{pr} is of order unity for particle radii of order 0.5 μm, or near where most of the solar energy is contained. Therefore, the important interactions begin to occur when the particle is roughly the same size as a characteristic wavelength of the incident solar spectrum. Unhappily, geometrical optics is therefore not valid in the region where the force becomes significant. The more general Mie calculation must be substituted for sizes smaller than about a micron.

Mie Calculations

The scattering of a plane, monochromatic electromagnetic wave of wavelength λ by a homogeneous isotropic sphere of known optical properties is described by Mie's solution to Maxwell's equations. Numerous tabulations of the energy absorbed and the energy scattered with its angular distribution have been given as functions of the size parameter $X \equiv 2\pi s/\lambda$ and the particle's optical properties; these are based on series expansions in X of analytical expressions (see, e.g., van de Hulst, 1957; Hansen and Travis, 1974). To find the radiation pressure felt by a real particle in interplanetary space, one needs to use the Mie solution to compute the optical efficiency factors corresponding to the different optical properties of the various wavelength regions and then to integrate these over the energy distributed in the actual solar spectrum.

A method of computing these integrals for spherical grains using the rigorous Mie theory has been previously described by Lamy (1974b, 1975), who also reviews the numerical techniques of other authors. We improve Lamy's earlier calculation in two ways:

(i) The domain of integration has been extended to 0.15–15 μm, the lower limit being taken in order to permit the inclusion of the sharp increase in the extinction coefficients of silicates in the ultraviolet. The integration accuracy has been bettered by reducing the size of the integration steps used in computation with the trapezoidal rule; they are now 0.01 μm from 0.15–0.4 μm, 0.02 μm from 0.4–0.7 μm, 0.05 μm from 0.7–1.0 μm, 0.1 μm from 1.0–6.0 μm, and 0.25 μm from 6.0–15.0 μm. Thus, the integrands are evaluated at 138 values in the wavelength range for each of thirteen grain sizes: $s = 0.005, 0.01, 0.05, 0.07, 0.1, 0.2, 0.3, 0.4, 0.5, 1.0, 3.0, 5.0,$ and 10.0 μm.

(ii) The mean solar flux $S(\lambda)$ at a distance of 1 AU is now obtained from the recent and extensive compilation of Vernazza *et al.* (1976) in the interval 0.15–0.4 μm. Beyond

0.4 μm their values appear too low and we rely on the data of Makarova and Kharitonov (1972) which represent a good average in the interval 0.4–1.0 μm and those of Arvesen et al. (1969) in the 1.0- to 2.0-μm domain. Further in the infrared we employed the brightness temperature values reported by Vernazza et al. (1976, Fig. 11). A total of 138 numerical values of $S(\lambda)$ were introduced to calculate the integrands.

Materials

The materials to be considered are chosen for several reasons. Briefly, we wish to study materials which might be typical of interplanetary dust and for which laboratory experiments have reasonably delineated the complex index of refraction in the wavelength interval of interest. In addition at least a few materials should represent each of the possible different optical classifications—some should be dielectrics, others conductors; some transparent, others very absorbent. As archetypes which have significant cosmic abundances, we choose several silicates, water ice, iron, magnetite, and graphite. The three silicates chosen are presumed to be representative of dust produced from asteroids and comets as well as that found in interstellar space (Day, 1977; Huffman, 1977): *obsidian,* a volcanic glass, is a good example of dirty fused quartz; *amorphous quartz* is chosen in preference to crystalline quartz because interplanetary grains appear to become amorphous (at least on their surfaces) by solar wind ion implantation (Bibring et al., 1974); and *basalt,* a rock made essentially from olivine, pyroxene, and feldspar, may be considered as representative of stony meteorites. *Water ice* is selected because of the expectation that it will be injected into interplanetary space by comets; solid water is chosen rather than liquid because particles of ice sublimate before reaching the melting point (Lamy, 1974a). *Iron* has a high cosmic abundance; it is found in many meteorites and has been invoked by Wolstencroft and Rose (1967) to explain the

polarization of the zodiacal light. *Magnetite* is a black isometric mineral (Fe_3O_4) often found in meteorites and captured interplanetary grains (Brownlee et al., 1976; 1977), and with other iron compounds as a residue lining lunar microcraters (Nagel et al., 1976); it is also considered a likely constituent of interstellar grains (Huffman, 1977). *Graphite,* a strong absorber of visible light, is introduced in connection with the interstellar grain problem (see Aannestad and Purcell, 1973; Knacke, 1977; and Huffman, 1977; but also Hoyle and Wickramasinghe, 1977) and because of its presence in carbonaceous chondrites. Lastly, we include a hypothetical *ideal absorbing material* as a comparison standard and also plot the radiation pressure as though the conditions of *geometrical optics* were satisfied for all particle sizes.

The specific complex indices of refraction for the materials considered here will be tabulated elsewhere (Lamy, in preparation; see Lamy, 1975) and so we limit ourselves to a brief mention of this topic. The majority of the optical data for amorphous quartz comes from Steyer et al. (1974), Malitson (1965), Heath and Sacher (1966) and Drummond (1935). For obsidian and basalt the results of Pollack et al. (1973), as recently extended into the ultraviolet by Lamy (1978), are employed. The index of refraction of ice at 100°K has been measured by Bertie et al. (1969), and already employed by Lamy and Jousselme (1976) in order to evaluate the temperature of interplanetary ice grains. The classical reference for the optical properties of graphite is Taft and Phillips (1965). The modern measurements of Huffman and Stapp (1973) and Steyer (1974) provide the optical properties of magnetite over the domain 0.09 to 100 μm. For iron, we use the optical properties as determined by Moravec et al. (1976) in the interval from 0.045 to 0.5 μm, by Gorban et al. (1973) from 0.25 to 1 μm, and by Lenham and Treherne (1966a,b) in the range 1 to 18 μm. Our "ideal particle" is one that absorbs all radiation for which

$X = 2\pi s/\lambda \geq 1$ but is totally transparent to longer radiation; it has been previously considered by Zook and Berg (1975). The geometrical optics example assumes Q_{pr} to always be unity.

Values of Radiation Forces

The relative radiation pressure force β as given by (19) with Q_{pr} evaluated by the Mie program is plotted in Figs. 7a and b as a function of particle size for the seven cosmically significant materials introduced above and for two comparison standards. Note that, except for graphite and conducting particles, the repulsive radiation pressure force never exceeds the attraction of gravity. This is in contradistinction to the popular view in which all particles smaller than a certain size are "blown" out of the solar system; nevertheless, as discussed later, a process exists whereby particles can be ejected from the solar system even

though $\beta < 1$. The conclusion that β remains less than unity for very small particles agrees with the existence of numerous lunar microcraters corresponding to impacts with particles at least as small as 0.05 μm or less. The numerical result of Figs. 7a and b further show that, since the radiation pressure and Poynting–Robertson drag are each linear in Q_{pr}, both these processes are insignificant for all very small particles.

The gross features of Fig. 7 can be physically interpreted. Toward this end we have plotted there two illuminating examples that provide standards for comparison. The first is the geometrical optics case ($Q_{pr} = 1$, $\rho = 3$ g cm^{-3}), for which $\beta = 0.19/s$ from (19) with s in μm. The result for the ideal material drops below the geometrical optics case for sizes shortward of about 0.3 μm, peaking at roughly 0.1 μm; this reflects the fact that the solar spectrum is maximum near 0.5 μm and is itself fairly narrow. For particles of any composition with sizes
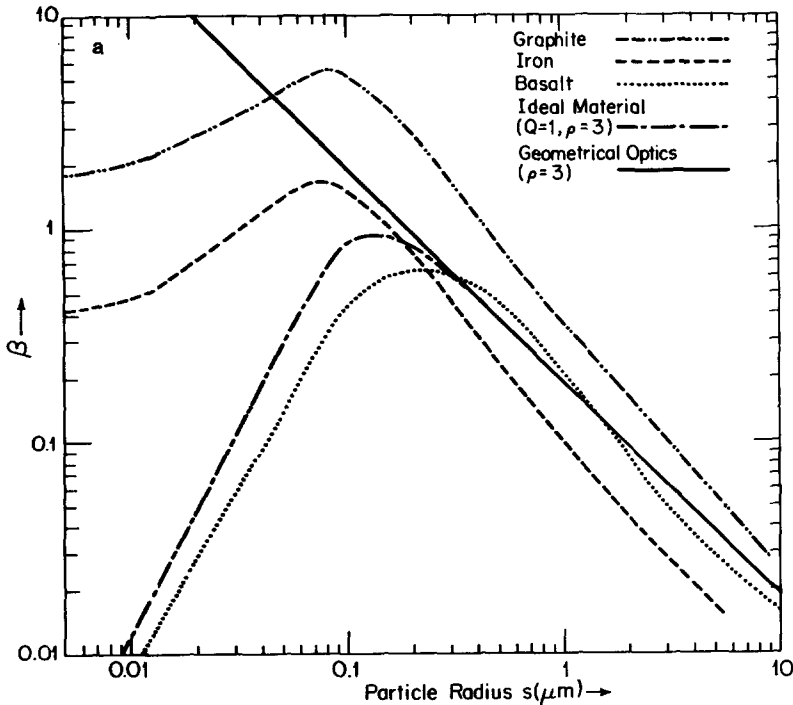

FIG. 7a. A log–log plot of the relative radiation pressure force $\beta = F_r/F_g$ as a function of particle size for three cosmically significant materials and two comparison standards. See text for discussion.
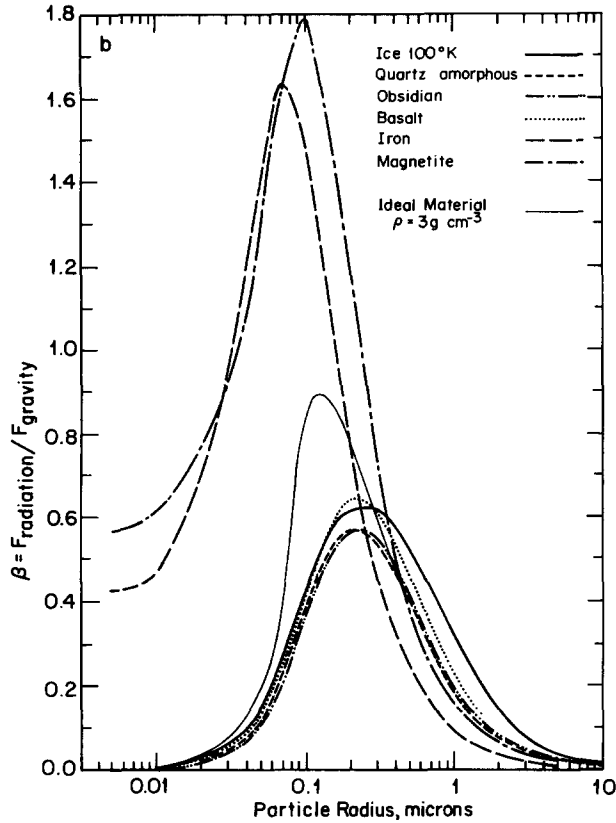
FIG. 7b. A semilog plot of the relative radiation pressure force $\beta = F_r/F_g$ as a function of particle size for six cosmically significant substances and an ideal material. See text for details.

greater than a few microns, geometrical optics holds, since most of the solar energy is concentrated in wavelengths near 0.5 μm. Thus Q_{pr} is essentially constant, independent of particle size, meaning that the β curves are linear on the log plot of Fig. 7a and hyperbolae, proportional to s^{-1}, in Fig. 7b; the different absolute values for the various materials are due to variations in particle density and albedo. At the other side of the figure, very small particles are virtually unaffected by the momentum in the solar radiation, because the characteristic radiation wavelength $\bar{\lambda}$ is relatively too large to sustain much absorption or scattering. Most curves peak near 0.1 μm, just as is the case for the ideal material: the important interactions are for particle sizes comparable to $\bar{\lambda}/2\pi$, decreasing sharply for smaller X, and

$\bar{\lambda}/2\pi$, for the solar spectrum is about 0.1 μm.

The metals suffer a large radiation pressure because they backscatter radiation ($\langle \cos\alpha \rangle < 0$) whereas the dielectrics are strong forward-scatterers. Graphite feels a relatively large radiation force for a variety of sizes because, due to its large imaginary index of refraction, it absorbs radiation over a wide wavelength range, very much like a metal, and hence even particles for which X is substantially less than unity absorb efficiently; because such particles have small mass, $\beta > 1$. Even though water ice is relatively transparent, its low density produces a curve similar to the dielectrics.

The numerical integrations are terminated at large particle sizes because so many terms are needed for the Mie series

expansions to converge (the number of terms goes roughly as X) that the computations become too expensive. For that matter one should be cautious about trying to accurately calculate the radiation pressure of any big particle by a geometrical optics approach: once particles become that large, the surface elements making up the "spheres" become scatterers themselves since they can be on the order of a characteristic wavelength.

One might hope that the small-size end of the β plot would be expressed by the Rayleigh scattering formula, $Q \propto s^4$ or $\beta \propto s^3$ (Jackson, 1962, p. 573). Unfortunately, although one requirement ($X \ll 1$) of the Rayleigh scattering approximation holds, the other $-|dX| \ll 1$ with d the refractive index, is less well satisfied; for example, considering iron particles of 10^{-2}-μm radius, $X = 10^{-1}$ but $|dX| \approx 0.4$. This inapplicability of the Rayleigh result is borne out in Fig. 7. At very small sizes where Rayleigh scattering might operate, complex quantum effects, which are not well understood (see Huffman, 1977), may need to be considered. There is a tendency, according to the Mie results, for β to approach a constant value in this region. Of course, at extremely small sizes (namely, an atom or two), atomic absorption becomes important and β can rise above zero; nevertheless this only is significant for hydrogen for which, due to the large amount of energy contained in the solar Lyman-α line, β is about 1.25.

Calculations of β similar to those shown in Figs. 7a and 7b have also been carried out by Öpik (1956), Shapiro et al. (1977), Singer and Bandermann (1967), Gindilis et al. (1969), Mukai and Mukai (1973), Lamy (1974a, 1974b, 1975), Schwehm (1976), and Rajan and Weidenschilling (1977), but we believe that the results presented here are more complete. Our numerical program is more precise and a more thorough search of the literature has been made to locate the optical properties of the materials in each particular wavelength region. Moreover we consider a range of materials which is proba-

bly more representative of interplanetary debris; however, carbonaceous chondritic materials should be added by subsequent workers. Our results do not differ significantly in character from those of previous authors with the exception of the early, and necessarily crude, models of Öpik (1956) and Shapiro et al. (1966). Singer and Bandermann (1967), Gindilis et al. (1969), Mukai and Mukai (1973), and Schwehm (1976) agree with the conclusions that (i) the radiation force is less than gravity for most materials, (ii) the maximum value of β generally occurs at a few tenths of a micron, (iii) metals differ in their response from dielectrics, and (iv) very small particles are virtually unaffected by the momentum carried by the radiation field.

The breadth and height of the result for graphite may be significant in two respects. First, the majority of captured dust particles are observed to be carbonaceous chondritic in composition (especially like $C1$ chondrites but having some similarities to $C2$ objects) and low in reflectivity (Brownlee et al., 1976, 1977). Such particles are known to have carbon abundances of a few percent. In light of the graphite curve, we wonder—and intend to check in a later publication—whether most small interplanetary particles are chondritic and are therefore particularly susceptible to radiation pressure. Second, graphite is one of the materials proposed as making up a substantial fraction of interstellar grains (Aannestad and Purcell, 1973; Huffman, 1977; Knacke, 1977) even though for cosmochemical reasons it should be less prominent than other materials. However, Fig. 7a suggests that graphite may be preferentially expelled from the neighborhood of stars. Moreover graphite is known to be formed about carbon stars, which are not especially massive, but are fairly luminous. It seems as though ejection should be favored unless the optical properties of graphite change in going to the longer wavelengths of these cool stars. This calls attention to the value of carrying out Mie calculations with accurate optical

properties similar to the above but for different stellar classes. Such calculations should be completed not only for graphite grains but also for water ice and silicate material; the former might account for interstellar absorption centered at 3 μm while the latter would produce the absorption feature near 10 μm. A start has been made on such calculations by Divari and Reznova (1970), Wickramasinghe (1972) as well as Lamy (1979, in preparation).

By their very definition Figs. 7a,b are valid only for particles in the present solar radiation field. If the solar luminosity has changed in the past, the entire suite of curves should be raised or lowered. Precisely how this occurs depends on the spectral irradiance $S(\lambda)$ and on $Q_{pr}(\lambda)$ for each specific material. For example, if the Sun passed through a more energetic T-Tauri phase, as suggested by many cosmogonists, then a wider range of particle sizes may have been blown out of the solar system; because such stars radiate mainly in the infrared, larger particles are more likely to have been ejected. Furthermore an enhanced stellar wind during the T-Tauri phase may dominate radiation effects. Nevertheless, as a result of the quite narrow peak in most β curves, only a relatively small class of particles would still be so affected. In this respect we note that microcraters are seen on the surfaces of small glass spherules found in the interior of the Kapoeta meteorite (Brownlee and Rajan, 1973) and perhaps in other meteorites. The character and size range of these microcraters are similar to those of contemporary lunar microcraters, so we have here an indication of the existence of very small particles in a meteorite which is thought to be about 4.0×10^9 years old. This may mean that the solar luminosity was not much different then. Any shift to shorter wavelengths in the peak of the solar energy spectrum, corresponding to higher surface temperatures, would accordingly move the peaks in the β curves to smaller sizes. This should also be the case for particles orbiting any star of roughly a solar mass: particles are more readily ejected by higher luminosity stars and, furthermore, particles of smaller sizes are more susceptible to ejection when placed near hotter stars. Lastly, fluffy particles or very irregular particles, which have large surface-to-mass ratios, suffer relatively greater values of β and thus are more likely to be affected by the solar radiation; it is improbable that particles of such morphology with sizes near 1 μm would be present in interplanetary space today if our calculations have any validity.

In general, due to the mass-luminosity relation $L \propto M^3$ for main sequence stars, we would expect that more massive stars are able to expel a wider composition and size range of dust particles. Calculations by Divari and Reznova (1970) show that this indeed appears to be the case.

VII. DYNAMICAL EFFECTS OF RADIATION PRESSURE

Abrupt Orbital Changes; Escape from the Solar System

Since the radiation pressure force is a radially-directed, inverse-square force like gravity, it alone does little to complicate the orbital dynamics of dust particles so long as its coefficient remains constant. With the introduction of radiation pressure, a particle's motion is now controlled by the net force, so that, ignoring the small Poynting–Robertson drag,

$$\ddot{\mathbf{r}} = -(1 - \beta)\mu\hat{\mathbf{S}}/r^2, \qquad (20)$$

where β is the ratio of radiation repulsion to gravitational attraction and $\mu \equiv GM$. Since the force remains radial and inverse square, the orbits are still conic sections. If $\beta < 1$, the net force is attractive and so elliptic, parabolic, and hyperbolic orbits are permitted, depending on the orbital energy. If $\beta > 1$, only hyperbolic orbits occur as in the case of electron–electron collisions.

We have seen that radiation pressure forces rarely exceed gravity. However, this does not necessarily mean that particles

cannot attain hyperbolic escape orbits. As first noted by Harwit (1963), and later considered by Whipple (1967), Dohnanyi (1972, 1978), Zook (1975), Zook and Berg (1975), Kresák (1976), and Rajan and Weidenschilling (1977), all that is necessary for ejection from the solar system is for a particle's specific orbital energy,

$$E/m = v^2/2 - \mu/r \equiv -\mu/2a, \quad (21)$$

to become positive; v is the particle velocity at solar distance r and a is the semimajor axis of the elliptical orbit. For particles unaffected by radiation, the orbital semimajor axis a is constant becaue E is conserved in a r^{-2} field. However, consider a small particle which is suddenly released from a much larger parent body: radiation pressure immediately comes into play and the particle's β undergoes an abrupt change from essentially zero (that of the parent body) to some finite value. Equation (21) still holds except that μ is replaced by a new value

$$\mu' \equiv \mu(1 - \beta); \quad (22)$$

if β is sufficiently large, E will be positive.

To illustrate the size of particles for which ejection becomes possible, consider a particle to be released at perihelion, where $r_p = a(1 - e)$ and $v_p^2 = (\mu/a)(1 + e)/(1 - e)$ for an orbit of eccentricity e. Ejection then occurs for $E \geq 0$, so that, from (21) and (22), particles for which

$$\beta_p \geq (1 - e)/2 \quad (23)$$

are placed on hyperbolic trajectories; the corresponding limit for aphelion ejection is $\beta_a \geq (1 + e)/2$ (Kresák, 1976; Rajan and Weidenschilling, 1977). Even particles on circular orbits ($e = 0$) need only have $\beta = \frac{1}{2}$ for ejection (cf. Zook and Berg, 1975). This is understandable qualitatively since the particle's velocity at the instant of release is governed by its motion *before* release, that is, by the motion of the large particle that experiences essentially no radiation force; after release the particle's motion is controlled by the forces it *then* feels. If the particle is of the proper size, following release

it may be moving too fast to be bound by the new potential field (i.e., μ'). Hence such particles are placed on hyperbolic orbits even though their $\beta < 1$. In fact, it is worth observing that $\beta_p \geq 10^{-5}$ is all that is required for solar system ejection from long-period comets, and even for Comet Halley it is only 0.016; these values make escape following release near perihelion quite plausible.

Any small particle produced close to a star can be accelerated to enormous radial velocities if it does not burn up first. Using conservation of energy [see (21)], we find that a particle introduced at distance r_0 with the initial velocity v_0 will have acquired, by the time it reaches a distance $\gg r_0$, a terminal velocity v_∞ given by

$$v_\infty^2 = v_0^2 + 2\mu(\beta - 1)/r_0. \quad (24a)$$

Thus a particle released from a long-period "Sun-grazing" comet at perihelion distance R_0 (measured in solar radii) will have a terminal velocity

$$v_\infty = v_{esc}(\beta/R_0)^{1/2}, \quad (24b)$$

where $v_{esc} = 617$ km/sec is the usual escape velocity from the surface of the Sun. For example, a particle with constant $\beta = 1$ released from such a comet at a perihelion distance of $R_0 = 10$ would have a velocity of nearly 200 km/sec when crossing the Earth's orbit. Its velocity when leaving the solar system would be the same, but the particle would become entrained with the local interstellar gas after moving only a few tens of light years. Even with $v_0 = 0$, the terminal velocity can be large if $\beta > 1$. Thus a hypothetical particle formed in a stellar atmosphere at R_0 stellar radii from the center will have a terminal velocity, neglecting drag forces, of

$$v_\infty = v_{esc}[(\beta - 1)/R_0]^{1/2}, \quad (25)$$

where v_{esc} is now the escape velocity from the surface of the particular star. A calculation of ejection velocities from two model cool stars is presented by Wickramasinghe (1972), who also discusses some conse-

quences of the energetic ejection velocities which result from this process.

Numerous particles on hyperbolic orbits, called β meteoroids by Zook and Berg (1975), appear to exist in interplanetary space (Berg and Grün, 1973). During seven years of data collection Pioneers 8 and 9 found many more particles to be streaming away from the Sun than moving toward it; Helios 1 observations (Grün et al., 1977) confirm this. These must be hyperbolic particles, for if they were on elliptic orbits they would eventually return to be recorded during their motion toward the Sun. Doppler shifts of the zodiacal light spectrum have been taken to show many scattering particles have orbital velocities greater than the local escape velocity (Fried, 1978). Further evidence for hyperbolic particles is the hint in the lunar microcrater data for two species of dust at very small particle sizes (Hörz et al., 1975; Brownlee et al., 1975; Morrison and Zinner, 1977; LeSergeant and Lamy, 1978); one class might be hyperbolic particles while the other would be the usual interplanetary dust. The hyperbolic trajectories of those β meteoroids, streaming out from the Sun's vicinity, which manage to impact the lunar surface must be confined more closely to the ecliptic plane. Thus the orientations of the lunar rock surfaces on which the two classes of microcraters are preferentially observed may be distinctive. This is currently unresolved with Morrison and Zinner (1975) and Mandeville (1977) not seeing any such effect, in disagreement with Hutcheon (1975) and Hartung et al. (1975).

Small particles may be instantaneously generated in interplanetary space in several possible ways. The most straightforward is by collisions between larger dust grains (Whipple, 1976; Zook and Berg, 1975; Dohnanyi, 1976a; Rhee, 1976); this process should be enhanced near the Sun since particle densities and orbital velocities are higher there (see, e.g., Zook and Berg, 1975, Fig. 2). Another production mechanism, already introduced, is for material to

be directly released from comets during heating near perihelion passage. Whipple (1967, 1976) believes that most dust comes from short-period comets, particularly Encke ($e = 0.847$) and Halley ($e = 0.967$); Sekanina and Schuster (1978) disagree. Delsemme (1976) finds long-period and new comets more productive. From the criterion derived above we see that material released from Encke at its perihelion will be ejected from the solar system if its $\beta > 0.08$, from Halley if $\beta > 0.016$, and from the average short-period comet ($\bar{e} = 0.56$) when $\beta > 0.22$. In all these cases, ejection from the solar system becomes a possibility for a much wider size range than classical ideas would imply. It is noteworthy that most meteor showers are associated with short-period comets, especially those of high e. In this case, the size of the "large" particles (those virtually unaffected by the radiation field) may be no more than a centimeter or so. Rapid sputtering and sublimation may produce similar phenomena for particles near 1 μm (Sekanina, 1976). A final mechanism to produce very small particles from larger ones is rotational bursting, in which small particles are spun up by radiation forces to such high angular velocities that the resultant centrifugal stresses exceed the tensile strength of the object; to accomplish this spin-up Radzievskii (1954) suggests a "windmill" torque driven by albedo variations while Paddack (1969; cf. Paddack and Rhee, 1976) proposes a "paddlewheel" torque caused by surface irregularities. Many of the above mechanisms invoke the breakup of large particles, drifting sunward because of Poynting–Robertson drag, to supply the source of the small particles which become β meteoroids: they are thus subject to considerations of mass flux conservation and, as LeSergeant and Lamy (1978) have argued for a particular model of the dust, these large particles may fail in producing sufficient outflow.

Lastly it should be noted that, if cometary particles are indeed fluffy, then $\beta > 1$ for some size range and direct ejection will

occur without the clever dynamics described above. In addition particles which condense in the atmospheres of cool stars may be rapidly ejected from the system if, shortly following nucleation, $\beta > 1$; that is to say, escape from these stars usually occurs before the particles have attained their maximum permitted condensation sizes, which may in part explain why interstellar grains are small.

Continuous Orbital Changes: Gradual Modification of Radiation Pressure

We have seen that the orbital energy of a small particle can be abruptly changed when it is detached from the parent body which had shielded it from the effects of radiation pressure. In such cases the particle departs along a simple conic section (perhaps a hyperbola), smoothly patched to that of its parent body. But a particle with β changing *continuously* will follow a more elaborate trajectory. This occurs most readily for particles sufficiently near the Sun to undergo gradual mass loss due to sputtering and/or sublimation.

One can write the orbital semimajor axis a and eccentricity e as functions of the orbital velocity $v = (\dot{r}^2 + H^2 r^{-2})^{1/2}$ and specific angular momentum $H = r^2\dot{\theta}$ (cf. Burns, 1976), which are themselves functions of the particle position (r, θ):

$$a = r/(2 - rv^2/\mu), \qquad (26)$$

$$e = (1 - H^2/\mu a)^{1/2}. \qquad (27)$$

In the typical orbital problem, $\mu = GM$ is the coefficient of the r^{-2} force but, once radiation pressure is included, it becomes $\mu' = GM(1 - \beta)$. Increasing the radiation pressure decreases μ' and thus the size of the orbit increases; it is as if the dust were attracted by a continuously less massive Sun.

The above expressions are convenient for considering cases in which μ' is not constant, such as can occur when the particle's size changes because of sputtering and/or sublimation/condensation (see Mukai *et al.*,

1974; Dobrovol'skii *et al.*, 1973; Lamy, 1974b), or when the stellar luminosity varies. The latter may be either apparent, as with the clearing of a circumstellar nebula (see Dorschner, 1971), or intrinsic, as with a variable or flare star. Differentiation of (26) and (27) with position and velocity constant yields

$$da/a = -a(v/\mu')^2 d\mu' \qquad (28)$$

and

$$de/e = [(H/\mu'e)^2/a](1 - a/r)d\mu'. \qquad (29)$$

From (22) and (28), we see that the orbital size always increases with increasing radiation pressure (i.e., for $d\mu' < 0$) and decreases as μ' becomes smaller. Similarly, the term $(1 - a/r)$ in (29) is negative near pericenter and therefore an increase in radiation pressure at that position causes a more eccentric orbit.

To compute the trajectory of a particle that is losing mass by sublimation requires a calculation of the sublimation rate (see Lamy, 1975), which is a strong function of the particle's temperature and surface properties, and involves the complex problem of sputtering. Here we merely illustrate an orbit that exhibits this behavior (see Lamy, 1974a, 1975, 1976b; Mukai and Mukai, 1973). We have chosen an obsidian particle, because then β is always less than unity (so it will not directly escape), and put it near the Sun to allow the sublimation to proceed rapidly. As shown in Fig. 8 the particle, after starting in a circular orbit, can be
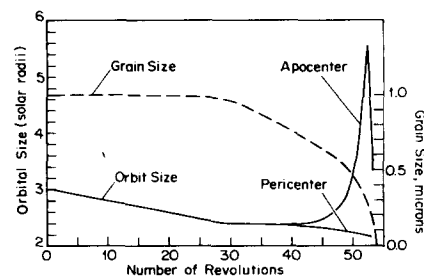
FIG. 8. The orbital evolution of an obsidian particle (initial size = 1 μm) near the Sun. The separating solid lines show aphelion and perihelion distances.

seen drifting slowly toward the Sun owing to the Poynting–Robertson drag; this drift will be computed later. The particle size is relatively constant until the temperature reaches a critical value at which the particle starts to sublimate quickly; the decrease in size accelerates as the temperature increases due to the growing proximity of the Sun. As the size approaches that at which β begins to be significant, the orbital character (a,e) changes. The orbit grows as the effect of (28) overbalances the Poynting–Robertson decay. At the same time, as seen by (29), the orbit also becomes eccentric. The pericenter continues to be dragged in but the rapid growth in apocenter, which would become infinite if $\beta \geq 0.5$, is halted once the particle shrinks to such a size that the maximum value of β is passed. The eccentricity then decreases because $d\mu'$ is now positive. Collapse continues under the effects of both Poynting–Robertson drag and decreasing a by virtue of (28). Before total orbital collapse can take place, the particle disappears: its lifetime is ended.

Continuous Orbital Changes: Effects of Perturbing Forces

We know that an inverse-square radial force field, like that of the gravity field of a spherical mass, produces orbits that are conic sections. Any small deviation from this ideal field, however, means that the orbits approximate, but differ slightly from, conic sections. To describe the manner in which the orbit is modified, we use the perturbation equations of celestial mechanics, which show the variation of the orbital elements with time under the action of a small perturbing force $\mathbf{dF}$ above and beyond the gravity force. If a particle in an elliptical orbit is suddenly subjected to such a perturbation, the particle's orbit is no longer elliptical; however an auxiliary orbit, the osculating orbit, may now be defined. This is the (elliptical) path that the particle would follow if $\mathbf{dF}$ suddenly vanished, say at $t = t_1$, and the particle continued along its way with $\mathbf{r}(t_1)$ and $\mathbf{v}(t_1)$ as initial conditions.

The orbital elements specifying the osculating orbit are the *osculating elements;* governed by the perturbation equations of celestial mechanics, these change slowly owing to $\mathbf{dF}$ and represent a gradually evolving orbit. This problem has been considered by celestial mechanicians for centuries. In place of more complicated techniques, Burns (1976) has simply derived the perturbation equations in terms of the disturbing force components by differentiating expressions for the orbital elements written in terms of the orbital energy and angular momentum per unit mass and then substituting for the manner in which the energy and angular momentum change with time under the action of the perturbation. He finds (after we correct two typographical errors) that the changes in the orbital elements of interest are

$$da/dt = -a\dot{E}/E = 2(a^2/mH)$$
$$[F_R e \sin f + F_T(1 + e \cos f)], \quad (30a)$$

$$de/dt = (e^2 - 1)(2\dot{H}/H + \dot{E}/E)/2e$$
$$= (H/m\mu)[F_R \sin f$$
$$+ F_T(\cos f + \cos \psi)], \quad (30b)$$

$$di/dt$$
$$= (\dot{H}/H - \dot{H}_z/H_z)[(H/H_z)^2 - 1]^{-1/2}$$
$$= (r/mH)F_N \cos \theta, \quad (30c)$$
and

$$d\omega/dt + \cos i(d\Omega/dt) = (H/m\mu e)$$
$$[-F_R \cos f + F_T \sin f(2 + e \cos f)/$$
$$(1 + e \cos f)], \quad (30d)$$

where $E = -\mu m/2a$ is the orbital energy, (F_R, F_T, F_N) are the (radial, transverse, normal) components of the perturbing force,

$$H = [a\mu(1 - e^2)]^{1/2}$$

is the angular momentum *per unit mass* and H_z is its component perpendicular to the reference plane (the plane above which i is measured), f is the particle's true anomaly and ψ its eccentric anomaly [$\cos \psi = (e + \cos f)/(1 + e \cos f)$], $\theta = \omega + f$ is the orbital longitude of the particle, and Ω is the longitude of node (see Fig. 9). To arrive at
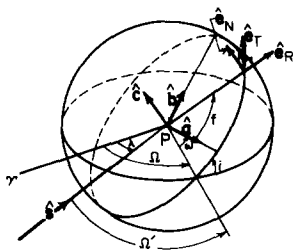
FIG. 9. Unit circle, centered on the planet P, showing the particle's orbit plane with inclination i relative to the orbital plane of the planet; ω is the argument of pericenter; Ω is the longitude of the node (measured relative to vernal equinox Υ, and $\tilde{\omega} = \omega + \Omega$ is that of the particle's pericenter; $\hat{a}$ is a unit vector from the planet to the orbit's pericenter; $\hat{b}$ also lies in the orbit plane, perpendicular to $\hat{a}$ and therefore points along the semiminor axis; $\hat{c} = \hat{a} \times \hat{b}$ and is parallel to $\hat{e}_N$. ($\hat{e}_R$, $\hat{e}_T$, $\hat{e}_N$) are the (radial, transverse, normal) unit vectors located at the particle whose true anomaly is f. The solar motion is given by $\lambda = n_\odot t$.

the secular change of the orbital elements, we take a and e to be constant over an orbit, assuming the perturbations are small, and time-average the perturbation equations. For example,

$$\langle \dot{a} \rangle = (1/P_0) \int_0^{P_0} \dot{a}\,dt$$
$$= (1/2\pi) \oint \dot{a}\,d\mathcal{M}, \quad (31a)$$

where $P_0 = 2\pi/n$ is the particle's orbit period and $\mathcal{M}$ is the mean anomaly, defined by $d\mathcal{M} = n\,dt$. Alternatively, we can integrate over the true anomaly f, using conservation of angular momentum, $H = r^2\dot{f}$, assuming it to hold over one orbit; thus,

$$\langle \dot{a} \rangle = (n/2\pi H) \oint \dot{a}r^2\,df. \quad (31b)$$

Orbits about Planets

Small particles are known to orbit the Earth. These probably come from several sources: (i) interplanetary meteoroid debris that was captured by the Earth during passage through its upper atmosphere, (ii) scattered lunar ejecta, and (iii) terrestrial materials that are randomly—although rarely—perturbed upward. Similar dust undoubtedly circles other planets, particularly those further out in the solar system, where it

may orbit on its own or as part of a planetary ring system. Soter (1971) has shown that some ejecta from impacts on the tiny Martian moons, which lie deep within their planet's gravitational potential well, can easily escape the satellites but find it much more difficult to leave the vicinity of Mars. As first pointed out by McDonough and Brice (1973), constituents of satellite atmospheres leak away from the satellites but remain in toroids centered around their orbits. Furthermore, sputtering by energetic magnetospheric particles kicks material off satellite surfaces into orbits about their planets; presumably this process accounts for the clouds of sodium and other elements observed near Io's orbit (Fang, 1976; Morrison and Burns, 1976; Brown and Yung, 1976). And now there is the possibility of volcanic gases being ejected by Io.

It is of some interest therefore to compute how the trajectories of planetocentric particles may be modified by radiation pressure, Poynting–Robertson drag and other forces. The redistribution of such material may provide an important loss mechanism, and may account in diverse ways for the unusual albedo patterns seen on the satellite systems of Jupiter and Saturn (cf. Pollack et al., 1978; Cruikshank, 1979). This problem has been addressed previously for Earth-orbiting dust (Shapiro et al., 1966; Peale, 1966; Lidov, 1969), for debris from Phobos and Deimos (Soter, 1971), and qualitatively for particles orbiting planets of the outer solar system by Morrison and Burns (1976) and by Mendis and Axford (1974), who emphasized the significance of electromagnetic forces. Poynting–Robertson decay times have been taken by Goldreich and Tremaine (1979) to place a lower bound on particle sizes in the Uranian ring system. Further discussion of the character of the orbital evolution of particles circling planets is given by Shapiro (1963) and Burns (1977); a simple review of the literature on this problem as pertaining to the motion of artificial satellites is provided by Sehnal (1969). Radiation forces on

particles in Saturn's rings are discussed by Lumme (1972) and Vaaraniemi (1973).

We investigate the motion of circumplanetary particles using the perturbation equations (30) of celestial mechanics described above. Compared to heliocentric orbits, planetocentric orbits present the added complication that the radiation unit vector $\hat{S}$ no longer lies exlusively in the particle's orbit plane. We must then average the perturbations over the parent planet's orbital period (i.e., the period of the motion of $\hat{S}$ relative to the particle's orbit plane) as well as over that of the particle. The vectorial celestial mechanics introduced by Herrick (1948) is well suited to this task; it has been profitably employed in the treatment of this problem by Musen (1960) and Allan (1961, 1962, 1967). The orthogonal coordinate system $(\hat{a}, \hat{b}, \hat{c})$ to be used is shown in Fig. 9, where the unit vectors $\hat{a}$ and $\hat{b}$ are directed along the major and minor axes, respectively, and where $\hat{c} = \hat{a} \times \hat{b}$ is normal to the orbit plane in the direction of the orbital angular momentum. Note that $\hat{b}$ is parallel to the particle's velocity vector at pericenter but antiparallel to that at apocenter. Also from Fig. 9, we see that

$$F_R = F_a \cos f + F_b \sin f,$$
$$F_T = -F_a \sin f + F_b \cos f, \quad (32)$$

and

$$F_N = F_c,$$

where $F_a = \mathbf{F} \cdot \hat{a}$, $F_b = \mathbf{F} \cdot \hat{b}$, and $F_c = \mathbf{F} \cdot \hat{c}$ are the components of the perturbing force $\mathbf{F}$ along the axes of our coordinate system.

The position of the orbital plane relative to inertial space is given by Ω, the longitude of the particle's orbital node measured with respect to vernal equinox; thus $\Omega' = \Omega - \lambda$ is the longitude with respect to the Sun-planet direction $\hat{S}$, where $\lambda = n_\odot t$ is the mean longitude of the Sun along its orbit. Then, if ω is the argument of pericenter, we find from the figure and spherical trigonometry that

$$\hat{a} \cdot \hat{S} = -\cos \Omega' \cos \omega$$
$$+ \sin \Omega' \sin \omega \cos i, \quad (33a)$$

$$\hat{b} \cdot \hat{S} = \cos \Omega' \sin \omega$$
$$+ \sin \Omega' \cos \omega \cos i, \quad (33b)$$

and

$$\hat{c} \cdot \hat{S} = -\sin \Omega' \sin i, \quad (33c)$$

where i is the inclination of the particle's orbit plane with respect to that of the planet. (For an equatorially orbiting particle, as in Saturn's rings, i is therefore the obliquity of the planet.)

In order to simplify the problem, we make the following assumptions: (i) Sunlight reflected from the planet's surface is ignored; numerical integrations by Shapiro (1963) show its effect to be small. (ii) The solar flux is taken to be constant, i.e., the planet's eccentricity is ignored; the mean motion $n_\odot$ then approximates the true angular motion of the Sun. Because the planetary orbit is assumed to be circular and because satellite orbits are small compared to those of planets, changes in the radiation forces as a particle approaches and then recedes from the Sun are negligible. (iii) Passage through the planetary shadow (see Fig. 10) is usually ignored; numerical integrations by Allen (1962) demonstrate that its inclusion does not modify the character of the perturbed motion but only decreases its magnitude, and then by at most tens of percent (see also Radzievskii and Artem'ev, 1962). Particularly for the more distant orbiting particles, it is unimportant. (iv) In-
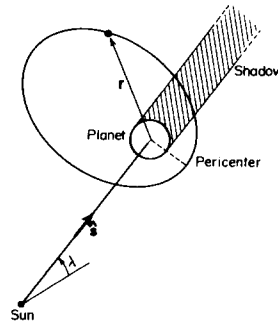

FIG. 10. Passage of particle through planetary shadow. The particle generally enters into, and emerges from, the shadow at different solar distances.

teractions with the planetary magnetic field are not considered (see Shapiro and Jones, 1961). (v) The planet is taken to be spherical, which means that resonance effects between, for example, orbital precession rates and the motion of the planetary shadow are not included (see Shapiro, 1963, and Allan, 1967); in addition the gravitational perturbations of planetary satellites are ignored.

Accepting these simplifications, we rewrite Eqs. (30) in terms of (32), so that

$$da/dt = 2(a^2/mH)[-F_a \sin f$$
$$+ F_b(e + \cos f)],$$
$$de/dt = (H/m\mu)[-F_a \sin f \cos \psi$$
$$+ F_b(1 - \cos f \cos \psi)],$$
$$di/dt = (r/mH)F_c(\cos \omega \cos f$$
$$- \sin \omega \sin f),$$
$$d\omega/dt + \cos i \, d\Omega/dt$$
$$= H[m\mu e(1 + \cos f)]^{-1}$$
$$[-F_a(1 + \sin^2 f + e \cos f)$$
$$+ F_b \sin f \cos f],$$

and we time average these rates over an orbit, as indicated in (31). Note that for radiation pressure,

$$F_a = F\hat{a} \cdot \hat{S}, \quad F_b = F\hat{b} \cdot \hat{S}, \quad F_c = F\hat{c} \cdot \hat{S},$$

where $F = (SA/c)Q_{pr}$; by the basic assumption of the perturbation technique, these are constant over an orbit. The time-averaged integrations of the first three are then most simply performed in the eccentric anomaly ψ, making use of the standard relations (cf. Danby, 1962, pp. 127 and 152)

$$d\mathcal{M} = (r/a)d\psi = (1 - e \cos \psi)d\psi, \quad (34a)$$

$$\sin f d\mathcal{M} = (1 - e^2)^{1/2} \sin \psi d\psi, \quad (34b)$$

$$\cos f d\mathcal{M} = (\cos \psi - e)d\psi. \quad (34c)$$

Thus we have

$$\langle da/dt \rangle = 0, \quad (35)$$

$$\langle de/dt \rangle = \tfrac{3}{2}(HF/m\mu)\hat{b} \cdot \hat{S}, \quad (36)$$

$$\langle di/dt \rangle = -\tfrac{3}{2}(aF/mH)(e \cos \omega)\hat{c} \cdot \hat{S}, \quad (37)$$

$$\langle d\omega/dt + \cos i \, d\Omega/dt \rangle$$
$$= -\tfrac{3}{2}(HF/m\mu e)a \cdot \hat{S}. \quad (38)$$

Equivalent expressions have been previously derived by Musen (1960), Bryant (1961), Allan (1962) and Chamberlain (1979).

We see first that the semimajor axis of a circumplanetary orbit is unchanged by radiation pressure. This happens because (30a) shows that work must be done on the orbit in order to affect a. In any conservative force field, work is only accomplished by absolute displacements through the field. A constant force field, such as the assumed solar radiation field, is a conservative force field and thus no work is done by it as long as, following one complete orbit, the particle returns to its initial position. But, according to the perturbation assumption, the particle *does* return to approximately where it had been and so the orbit size is unchanged. This ignores the likelihood that the orbit passes through the planetary shadow, entering into and emerging from it at different projected distances $\hat{r} \cdot \hat{S}$ (see Fig. 10). Thus, generally, work can in fact be done over a single orbit. Nevertheless, since the orbit precesses in its orbit plane under the action of radiation pressure (see below), all possible shadow orientations are sampled after the longitude of pericenter has rotated through 2π. Thus, even including shadowing (as long as resonance effects are ignored), the integrated result of the radiation force on the orbit size adds to zero when taken over enough orbits.

Next we note from (36) that changes in the eccentricity vary with the period of $\hat{b} \cdot \hat{S}$, that is, of the sine of the angle between the solar direction and the line of apses. It is therefore periodic both with the parent planet's orbital motion and with the motion of pericenter relative to inertial space; it is the motion of pericenter, under the combined action of radiation pressure and planetary oblateness, that allows resonance effects to come into play. However, if other perturbations are ignored, the motion of pericenter is a function only of the parent planet's motion, as we shall see, and thus $\langle de/dt \rangle$ has the period of the planetary

orbit alone. The maximum value of $\langle de/dt \rangle$ occurs when $\hat{b} \cdot \hat{S} = 1$, i.e., when the particle's velocity at pericenter is parallel to that of the incident sunlight. In contrast, when the particle is heading directly into the incident beam at pericenter, $\langle de/dt \rangle$ is most negative. All of these statements can be easily understood from the left-hand portion of (30b) which, since the orbital energy is conserved under radiation pressure forces [compare (30a) and (35)], reads $\dot{e} = -\dot{H}/eH$ for small e. The change in the magnitude of the angular momentum is the torque rF_T; when time averaged over an orbit, this in general is nonzero because the elongation of the orbit (see Fig. 10) gives a smaller moment arm at pericenter and the time spent there is less too. The time-averaged torque will be most positive (i.e., $\langle \dot{e} \rangle$ most negative) when the line of apses is normal to the solar radiation direction, with a leading $\hat{S}$. The periodicity of $\langle \dot{e} \rangle$ occurs simply because $\dot{H}$ is periodic since the planet progresses along its orbit and the dust particle's orbit reorients.

Finally, we see from (33c) and (37) that i changes most rapidly when it is large. This, in conjunction with the expectation that most sources of circumplanetary debris lie at low inclinations, implies that inclinations are small during most of the particle's lifetime (cf. Peale, 1966). Hence, we choose $\cos i \approx 1$ and therefore, from (33b) and (36),

$$\langle de/dt \rangle \approx n_\odot Z(\sin \bar{\omega} \cos \lambda$$
$$- \cos b\bar{\omega} \sin \lambda), \quad (39)$$

where $n_\odot = d\lambda/dt$ is the mean motion of the parent planet about the Sun, $\bar{\omega} = \omega + \Omega$ is the longitude of pericenter, and

$$Z = \tfrac{3}{2}[a(1 - e^2)/\mu]^{1/2}F/mn_\odot. \quad (40)$$

Furthermore, making the same approximation of low inclination, we have from (33a) and (38)

$$\langle d\omega/dt + \cos i d\Omega/dt \rangle$$
$$\approx d\bar{\omega}/dt \approx +(n_\odot Z/e)(\cos \bar{\omega} \cos \lambda$$
$$+ \sin \bar{\omega} \sin \lambda). \quad (41)$$

We can obtain approximate solutions to (39) and (41) by assuming Z to be constant, i.e., by neglecting terms of order e^2. We then introduce the new variables

$$h = (e/Z) \sin \bar{\omega}, \qquad k = (e/Z) \cos \bar{\omega},$$

so that

$$e^2 = Z^2(h^2 + k^2)$$

and

$$\dot{e} = Z(\dot{h} \sin \bar{\omega} + \dot{k} \cos \bar{\omega}).$$

Comparing with this (39) and (41), we have the equivalent equations

$$\dot{h} = n_\odot \cos \lambda, \qquad \dot{k} = -n_\odot \sin \lambda,$$

which, integrated from (h_0, k_0) at $\lambda = 0$ (i.e., $t = 0$), yield

$$h = h_0 + \sin \lambda, \qquad k = k_0 - 1 + \cos \lambda.$$

These solutions are substituted above to give

$$e^2 - e_0^2$$
$$= 2Z^2[(1 - k_0)(1 - \cos \lambda) + h_0 \sin \lambda].$$

If we specify that $t = 0$ when $\bar{\omega}_0 = 0$ (i.e., time starts at pericenter passage through the subsolar direction; as seen directly below, this is not restrictive), then $h_0 = 0$, $k_0 = e_0/Z$ and so

$$e^2 - e_0^2$$
$$= 2Z^2(1 - e_0/Z)(1 - \cos n_\odot t). \quad (42a)$$

In addition,

$$\tan \bar{\omega} = h/k = \sin n_\odot t/$$
$$(\cos n_\odot t - 1 + e_0/Z); \quad (42b)$$

it was this variation in pericenter location that was invoked earlier to claim that the planetary shadow samples all pericenter orientations. From this expression (plotted in Peale, 1966, Fig. 3), we see that the longitude of pericenter moves at a nonuniform rate; nevertheless, since the orbit spends the same amount of time at an orientation $\bar{\omega} - n_\odot t$ as it does at $-(\bar{\omega} - n_\odot t)$, the effect on $\langle \dot{a} \rangle$ of passing through the planetary shadow integrates to zero (see Fig. 10).

From (42) we see that the eccentricity oscillates with the planetary orbital period and has a characteristic amplitude $\sim Z$. As first pointed out by Peale (1966), this means that a particle in the size range that suffers significant perturbations can develop an eccentricity during its planet's orbit period sufficient to cause its elimination by collision with the planet. The maximum eccentricity that can be attained before a collision occurs is $e_{max} = 1 - R_p/a$, where R_p is the planet's radius.

The solution (42) describes the general periodic nature of the perturbation on e for small and moderate values of e, but it cannot formally be applied in the region of greatest interest (where e approaches unity) because, from (40), Z then is not constant and in fact can vanish. We therefore derive another approximate solution but one that applies in the region of large eccentricity. From (19) and (36), we can write the perturbation equation

$$\langle de/dt \rangle = \tfrac{3}{2}[a(1 - e^2)/\mu]^{1/2}(F/m)\hat{\mathbf{b}} \cdot \hat{\mathbf{S}}$$
$$= \tfrac{3}{2}(1 - e^2)^{1/2}\beta n_\odot(v_\odot/v)\hat{\mathbf{b}} \cdot \hat{\mathbf{S}}, \quad (43)$$

where $v_\odot$ and v are the mean orbital velocities, respectively, of the planet around the Sun and the particle around the planet.

Although e_{min} may be quite small (e.g., in the case of a particle ejected at low velocity from a satellite with small eccentricity), in most cases $e_{min} \neq 0$. However, in order to obtain an upper limit on e_{max}, let us assume that $e = 0$ at $t = 0$ and that e has its maximum value e_{max} at $t = \tfrac{1}{2}P_0$. Then integrating (43) between these limits,

$$\sin^{-1} e_{max} = \tfrac{3}{2}\beta(v_\odot/v)n_\odot\tau,$$

where

$$\tau = \int_0^{P_0/2} \hat{\mathbf{b}} \cdot \hat{\mathbf{S}} \, dt.$$

Since $0 < \hat{\mathbf{b}} \cdot \hat{\mathbf{S}} < 1$ when e is increasing, we have $\tau < \tfrac{1}{2}P_0$, so that

$$e_{max} < \sin [\tfrac{3}{2}\pi\beta(v_\odot/v)]. \quad (44)$$

The largest admissible eccentricity is of course $e_{max} = 1$, before which point the

particle must have collided with, or escaped from, the planet. A lower limit on β for elimination of a particle (having a *mean* circumplanetary velocity v) in this way can be found by assuming that an ideal alignment ($\hat{\mathbf{b}}$ parallel to $\hat{\mathbf{S}}$) is maintained throughout time $P_0/2$. Then, for e to reach 1,

$$\beta_c = \tfrac{1}{3}(v/v_\odot). \quad (45)$$

For a more normal motion of pericenter, β would have to exceed this limit, probably by a factor of several. Thus $\beta \geq \beta_c$ is a *necessary* condition for a particle to have the possibility to be lost from circumplanetary orbit by radiation pressure-induced perturbations of its eccentricity. We emphasize, however, that the possibility of elimination does not mean the certainty of loss: it all depends on the coupling between e and $\tilde{\omega}$ variations. This is a subject meriting further study. Preliminary results (Halamek and Burns, unpublished, 1979), based on numerically integrating the complete equations of motion, suggest that ejection is assured, regardless of initial conditions, once $\beta > (2 \text{ or } 3)\beta_c$.

Consider now the case of a particle ejected from a planetary satellite (by a cratering impact, say). Since most impact ejecta that escape the satellite will have velocities not much larger than the minimum escape velocity, we assume that the particle's initial circumplanetary orbit has low eccentricity and a velocity v nearly the same as that of its parent satellite. We see from (45) that, for a given planet, such a particle ejected from an inner satellite (with higher orbital v) requires a larger β in order to be in a position to be eliminated than does a particle from a more distant satellite. Thus, for example, a particle ejected from one of the outermost satellites of Jupiter (with $a/R_p \gtrsim 300$) stands a much better chance of developing a large eccentricity and thereby colliding with Jupiter or escaping the system than does an identical particle ejected from the innermost satellite ($JV, a/R_p = 2.55$). This is because it has less

orbital energy and so is more readily per- turbed by radiation pressure than is a parti- cle orbiting deeper in the planet's potential well. It is worth pointing out that the proba- ble loss flows for debris from the inner and the outer satellites can be in quite different directions if the criterion for ejection is only barely satisfied. For the former case, as e builds up but well before it reaches 1 (when escape occurs), the particle will strike the planet since then e need only be $1 - R_p/a$; that is to say, essentially all the debris from Amalthea will strike Jupiter. The same is not true for debris from an outer satellite since then $R_p/ \ll 1$; in this circumstance, half the particles will strike the planet (i.e., those that reach $e \approx 1$ when on their way into the planet) while the other half escape into solar orbit.

For particles ejected from solar system satellites in this way, the range of values of $\frac{1}{3}(v/v_\odot)$ is from 0.011 for the Moon to 0.676 for Amalthea. Referring to Fig. 7, this means that lunar ejecta with ~ 0.02 μm $< s < \sim 5$ μm may collide with the Earth or escape in less than 6 months after ejection from the Moon (unless it is strongly perturbed by, or previously collides with, the Moon), while only particles in a more restricted range (0.02 μm $< s < \sim 0.3$ μm for selected compositions) ejected from Amalthea can be eliminated in an analogous manner. We note that many of these parti- cles, even though they easily and rapidly escape from their circumplanetary orbits, may have heliocentric orbits that are only little modified by radiation forces. Because β_c must be exceeded by a factor of several for ejection, it is likely that debris from Amalthea or from one of the planetary ring systems cannot escape to interplanetary space; nevertheless it may be able to strike the parent planet.

Any particle with radiation pressure too weak to allow its rapid elimination by ec- centricity perturbations will remain in cir- cumplanetary orbit but will be subjected to the long-term Poynting–Robertson drag as described in the next section. This reduces its orbital semimajor axis which in turn les- sens the amplitude of the radiation pressure-induced eccentricity excursions (44) because v is increasing. Since the Poynting–Robertson drag induces no ec- centricity variation on its own, this means that such a particle will slowly spiral in to- ward the planet with ever diminishing maxi- mum eccentricity until it collides with an inner satellite or at last with the planet it- self. However, if solar wind (or magneto- spheric plasma) sputtering is sufficiently rapid, a large particle, originally little af- fected by radiation pressure, may be de- creased in size enough to enter the regime in which radiation pressure will pump up its eccentricity and thereby limit its lifetime. On the other hand, sputtering may directly cause the demise of very small particles be- fore their orbits collapse onto the planet.

Bertaux and Blamont (1973) have shown through numerical experiments that the radiation pressure produced by solar Lyman-α radiation striking circumterrest- rial hydrogen atoms, for which $\beta \approx 1.25$ during average solar conditions, causes rapid distortion of their orbits. Many atoms placed at a few Earth radii are lost in times as short as a few days; this may account for the depletion of hydrogen atoms observed by OGO 5 on the day side. Furthermore, they find that some particles placed at $20\,R_\oplus$ can be lost from the system by being trans- ferred to hyperbolic trajectories. This is of considerable interest to our earlier studies on orbital size and points out that highly perturbed particles which are loosely bound to their primary can be lost if they gain enough energy on the outbound first half of their circumplanetary orbit or if they gain enough angular momentum [cf. Eq. (45) which for this circumsterrestrial case would say ejection is possible if $\beta \gtrsim 0.1$] over the first half of their planet's orbit about the Sun. Moreover, even particles making sev- eral orbits of their primary could escape if, due to a particular orientation of the starting orbit, the shadow effect displayed in Fig. 10 happened fortuitously to continuously add

energy during the first half of the planet's orbit about the Sun. In each of these cases the orbital energy gained would have been ultimately lost from the orbit had the entire cycle been completed but, before the processes reversed to finish the cycle, the particle escaped and so was not there to benefit from the second half of the cycle.

Chamberlain (1979), in an analytical investigation of the possibility that radiation forces might redistribute circumterrestrial hydrogen atoms, disputes some conclusions of Bertaux and Blamont (1973). He does not address the issue of direct escape of atoms, because his interest lies with planetary exospheres whose particles, being nearby the planet, are first lost by collisions into its atmosphere. His results suggest three main effects: (a) high-inclination, eccentric orbits move swiftly to the ecliptic plane; (b) pericenters of direct orbits drift rapidly toward stable locations roughly westward (but eastward for retrograde orbits) of the planet; and (c) satellite orbits near such stable points are quickly eliminated by collision with the planet's atmosphere through a lowering of their pericenters. The analysis however does not include the solar motion.

The higher average eccentricity caused by radiation forces also means that collisions with satellites become more probable. The movement of dust particles between the Martian satellites due to radiation forces has been considered by Soter (1971). Soter (1974) also showed that, under the action of these forces, debris eroded from Phoebe, the retrograde outermost satellite of Saturn, could be streaming into the leading hemisphere of Iapetus, thus accounting for the latter's brightness asymmetry (cf. Cruikshank, 1979; Pollack et al., 1978). The important criterion for whether collisions occur by this mechanism is a comparison of the collision time between two orbiting particles found by the technique of Öpik (1951) with the drift time under Poynting–Robertson drag [see next section, especially Eq. (55)].

VIII. DYNAMICAL CONSEQUENCES OF POYNTING–ROBERTSON DRAG

Heliocentric Orbits

We note in (5) that the Poynting–Robertson force is in the opposite direction to the particle velocity. This takes both energy and angular momentum from the particle orbit, decreasing both the orbital semimajor axis and the eccentricity. To compute the consequences of these changes we return to the perturbation equations of celestial mechanics; the perturbation forces per unit mass for our problem are given by (6). The radial and transverse parts of the Poynting–Robertson acceleration are $F_R = -2(SAQ_{pr}/mc^2)\dot{r}$ and $F_T = -(SAQ_{pr}/mc^2)r\dot{\theta}$, respectively, where $S = S_0(r_0/r)^2$ is the solar flux at distance r from the Sun. There is no normal force component, demonstrating immediately by (30c) that there is no change in the orbital inclination for a heliocentric particle under the action of radiation pressure and Poynting–Robertson drag. The secular changes in a and e can be found by substituting F_R and F_T into (30) and time averaging the resulting expressions for $\dot{a}$ and $\dot{e}$, as in (31a), using

$$\dot{r} = [\mu/a(1 - e^2)]^{1/2}e \sin f \quad (46a)$$

and

$$r\dot{\theta} = [\mu/a(1 - e^2)]^{1/2}(1 + e \cos f) \quad (46b)$$

from Burns (1976). This procedure then yields

$$\langle da/dt \rangle = -(\eta/a)Q_{pr}(2 + 3e^2)/(1 - e^2)^{3/2} \quad (47)$$

and

$$\langle de/dt \rangle = -5/2(\eta/a^2)Q_{pr}e/(1 - e^2)^{1/2}, \quad (48)$$

where

$$\eta = S_0r_0^2A/mc^2 = 2.53 \times 10^{11}/\rho s \quad (49)$$

for spherical particles, with ρ and s in cgs units. Because the perturbing forces lie in

the orbit plane, the only other secular variation of an orbital element is the advance of perihelion whose change, even accounting for relativistic effects, is much slower than the variations of a or e (Wyatt and Whipple, 1950). The orbital parameters of cosmic dust particles detected by Pioneers 8 and 9 compare favorably with those expected if the particles had evolved due to Poynting–Robertson drag (Weidenschilling, 1978).

Except for the coefficient Q_{pr}, these expressions are identical to those derived by Wyatt and Whipple (1950), who considered Robertson's totally absorbing particle. They are also, with a redefinition of some coefficients, the same as the dynamical equations investigated by Donnison and Williams (1977a,b) who investigated the orbits of perfectly absorbing and perfectly scattering particles moving through the solar wind. Notice that in the limit of small eccentricity, the decay rate for e is $\frac{5}{4}$ that for a. The characteristic orbital decay time with $e = 0$ is easily found by integrating (47):

$$t_{\text{P-R}} = a^2/4\eta Q_{pr} = 7.0 \times 10^6 s\rho R^2/Q_{pr} \text{ years}$$

$$= 400 \, R^2/\beta \text{ years}, \tag{50}$$

where R is a measured in AU. It is readily shown that a^2/η is the time it takes for a particle at a to be struck by its own equivalent mass in solar radiation; that the collapse time is of the same order as, but smaller than this, is understandable in light of our view that the Poynting–Robertson drag results from the absorption of mass but not momentum.

The integration of da and de for finite e is not so simple but can be accomplished in closed form as shown by Wyatt and Whipple (1950); their results, when divided by Q_{pr}, produce characteristic Poynting–Robertson lifetimes for very small particles that become long, contradicting classical notions.

However, the inclusion of solar wind drag [see Section V, Eq. (17*)] will considerably shorten these times, since the drag due to the particulate radiation dominates that produced by electromagnetic radiation at particle sizes less than about a tenth of a micron. This is shown in Fig. 11, which gives the ratio of these drags as a function of size for an obsidian grain located at 1 AU. The actual ratio varies somewhat owing to changes in the solar wind characteristics with heliocentric distance and with time; of particular importance in the latter variations are sporadic solar storms whose effects are averaged in this plot. The drag ratio is small (of order 10^{-1}) and constant for particles larger than a micron or so since the collision cross sections of the dust grain to radiation and to the solar wind particles are the same and essentially invariant with respect to particle size (since geometrical optics holds for both).

The minimum at a size somewhat less than a micron reflects the growth in $\beta(s)$ relative to the geometric optics result in the same region (see Fig. 7a). The drag ratio increases at sizes smaller than this since Q_{pr} is unity for particle collisions, whereas it is
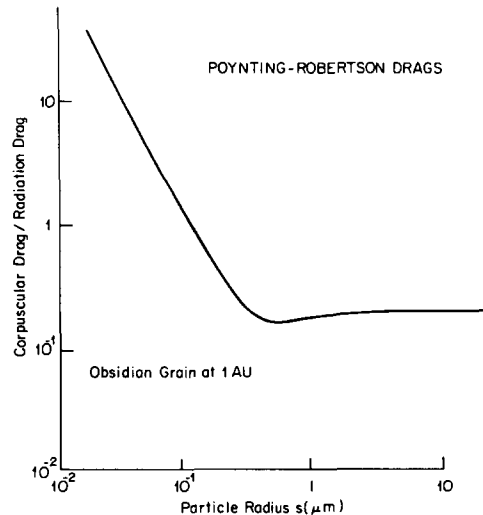

FIG. 11. Ratio of drag caused by the solar wind to that due to radiation on an obsidian grain at 1 AU. Based on a similar plot given by Lamy (1975).

much less than one for the photons, as seen in Figs. 7a and b. The slope of the line in this area differs for the various materials, owing to the specific optical properties of each substance. Of course when dust grains comprised of only a few hundred atoms or less are considered, then our model of a steady small drag is over-idealized; in such a case the momentum transfer to the particle is infrequent, abrupt, and relatively large in comparison to the grain's momentum.

We note in (50) that $t_{P-R} \propto \beta^{-1}$ and therefore from Fig. 7 that there should be a preferential removal of particles in the size range 0.02–1 μm due to the hastier collapse of the orbits of such particles. The lunar microcrater data do indeed show a deficiency: for example, lunar rocks 60095 (Brownlee et al., 1975), 12054 and 76215 (Morrison and Zinner, 1977), as well as five other rocks (Hörz et al., 1975), lack in a relative sense microcraters of pit diameter ~5–10 μm, corresponding to a projectile radius in the range 2–10 μm (Mandeville and Vedder, 1971), if one accepts that the laboratory simulation of collision by polystyrene into soda-lime glass at 5–14 km sec^{-1} is an appropriate analog (cf. Vedder and Mandeville, 1974). Unfortunately the difference in the observed and the modeled size ranges appears too large to be explained by Poynting–Robertson loss. Instead it could be that the deficiency of particles smaller than 10 μm is the immediate consequence of the ejection from the solar system by radiation pressure, as previously mentioned. Chernyak (1978) has suggested rather that such particles could have been vaporized during their passage through an earlier, now-extinct, lunar atmosphere. Or the relative absence of 1- to 10-μm particles could simply be a fact of nature, if LeSergeant and Lamy (1978) are correct in their belief that two independent dust populations, both of which have low number densities in the 1- to 10-μm region, exist.

The rate of loss by Poynting–Robertson spiralling has been used by several authors to compute the rate at which sources must supply the particles producing the zodiacal light. The most fundamental way of doing this calculation, originally devised by Whipple (1955), is to use conservation of mass and find out how rapidly particles are being lost from the system. Besides Poynting–Robertson collapse, the destruction of particles by collisions or sublimation, and the ejection of particles by radiation pressure must also be taken into account. To estimate the Poynting–Robertson loss, Whipple (1955) calculated the energy contained in the scattered sunlight and directly related this to the energy lost by the decaying orbits of the particles. This approach bypasses any computation of the dynamics and shows that Poynting–Robertson drag eliminates about 10^6 g sec^{-1}. However, not too much weight ought to be given to the precise loss rate since the integrated flux of zodiacal light was merely estimated and since Whipple's model implicitly assumes the only particle orbits are slowly decaying ellipses. For comparison a recent dynamical calculation (LeSergeant and Lamy, 1978) indicates a mass efflux of 3×10^4 g sec^{-1} for particles larger than 2 μm assuming a particle size distribution based on lunar microcrater data; this could be produced by about 10 short period comets like Encke or d'Arrest (Sekanina and Schuster, 1978a,b) each year. Whipple (1955) proposes that other effects, in particular Jupiter's perturbations and collisional destruction, are likely to be even more important than the Poynting–Robertson effect in removing particles.

Planetocentric Orbits

Any calculation of the effects of the Poynting–Robertson force on the orbit of a circumplanetary particle has to account for the fact that $\hat{S}$ does not in general lie in the orbit plane. We again use the vectorial celestial mechanics approach, applied above to the orbital evolution of circumplanetary particles acted on by radiation pressure, and invoke the same simplifications. In ad-

dition we employ the eccentric anomaly ψ which, from $r = a(1 - e \cos \psi)$ and $nt = \psi - e \sin \psi$, has a time derivative $\dot{\psi} = na/r$, where n is the particle's mean motion. In terms of the vectors $\mathbf{a} = a\hat{\mathbf{a}}$ and $\mathbf{b} = a(1 - e^2)^{1/2}\hat{\mathbf{b}}$ (see Fig. 9), it is readily shown (Allan, 1962) that $\mathbf{r} = \mathbf{a}(\cos \psi - e) + \mathbf{b} \sin \psi$ and

$$\dot{\mathbf{r}} = \dot{\psi}(-\mathbf{a} \sin \psi + \mathbf{b} \cos \psi). \quad (51)$$

The Poynting–Robertson force, being the velocity dependent part of (5), may be written

$$\mathbf{F}_{P-R} = -(SA/c^2)Q_{pr}[(\hat{\mathbf{r}} \cdot \hat{\mathbf{S}})\hat{\mathbf{S}} + \dot{\mathbf{r}}]. \quad (52)$$

Then the rate of change of a circumplanetary particle's orbital energy is

$$\begin{aligned}
\dot{E} = \mathbf{F}_{P-R} \cdot \dot{\mathbf{r}} &= -(SA/c^2)Q_{pr}[(\dot{\mathbf{r}} \cdot \hat{\mathbf{S}})^2 + \dot{\mathbf{r}} \cdot \dot{\mathbf{r}}] \\
&= -(SA/c^2)Q_{pr}\dot{\psi}^2[(\mathbf{a} \cdot \hat{\mathbf{S}})^2 \sin^2 \psi \\
&\quad + (\mathbf{b} \cdot \hat{\mathbf{S}})^2 \cos^2 \psi - 2(\mathbf{a} \cdot \hat{\mathbf{S}})(\mathbf{b} \cdot \hat{\mathbf{S}}) \\
&\quad \sin \psi \cos \psi + a^2(1 - e^2 \cos^2 \psi)].
\end{aligned}$$

This must now be time averaged over the particle's orbital motion (ψ), its advance of pericenter (ω), and the (assumed circular) orbital motion of its parent planet (Ω'). The averaging integrations of $\dot{E}$ can be performed in any order, but to obtain all expressions in closed form it is convenient to take ω and Ω' first. The dependence of $\dot{E}$ on ω and Ω' is through $(\mathbf{a} \cdot \hat{\mathbf{S}})$ and $(\mathbf{b} \cdot \hat{\mathbf{S}})$, and from (33) we have

$$\langle(\hat{\mathbf{a}} \cdot \hat{\mathbf{S}})^2\rangle_0 = \langle(\hat{\mathbf{b}} \cdot \hat{\mathbf{S}})^2\rangle_0 = \tfrac{1}{4}(1 + \cos^2 i),$$
$$\langle(\hat{\mathbf{a}} \cdot \hat{\mathbf{S}})(\hat{\mathbf{b}} \cdot \hat{\mathbf{S}})\rangle_0 = 0,$$

where $\langle \ \rangle_0$ indicates a quantity averaged over both ω and Ω'. Then

$$\begin{aligned}
\langle\dot{E}\rangle_0 = &-(SA/4c^2)Q_{pr}(a\dot{\psi})^2 \\
&(5 + \cos^2 i)(1 - e^2 \cos^2 \psi).
\end{aligned}$$

We finally average this last expression over the particle's orbital motion ψ, using (31a) and (34a), to obtain

$$\langle\dot{E}\rangle = -(SA\mu/4ac^2)Q_{pr}(5 + \cos^2 i), \quad (53)$$

where $\langle \ \rangle$ indicates the compound average. From (30a), $\langle\dot{a}\rangle = 2a^2\langle\dot{E}\rangle/\mu m$, where m is the particle's mass, so we have

$$\langle\dot{a}a\rangle = -\tfrac{3}{8}(S_0/R^2c^2)$$
$$(Q_{pr}/\rho s)(5 + \cos^2 i), \quad (54)$$

where $S_0 = 1.36 \times 10^6$ ergs cm^{-2} sec^{-1} is the solar constant and R is the heliocentric distance in AU. Similar results are available in Shapiro (1963), Peale (1966), and Allan (1967). We note that $\dot{a}$ does not contain e, unlike the heliocentric case, and that (54) is independent of orbital size. Integrating (54), we can write the exponential decay time for circumplanetary particles with $i = 0$ as

$$\tau_{P-R} = 9.3 \times 10^6 R^2 \rho s/Q_{pr} \text{ years} \quad (55)$$

with ρ and s in cgs units. For small particles it is more convenient to express this as

$$\tau_{P-R} = 530 \, R^2/\beta \text{ years},$$

using (19); β remains the ratio of radiation pressure to *solar* gravity. This ratio for planetocentric orbit collapse is essentially the same as (50), that for heliocentric orbit collapse; fundamentally this results because the Poynting–Robertson drag is due to the reradiation of the absorbed energy, which is nearly the same regardless of whether the planet or the Sun is being orbited. The slight difference in the coefficients is principally due to one being a characteristic decay time while the other is the integrated collapse time. Even though this collapse time can be short, the loss of *highly* perturbed circumplanetary particles more commonly happens due to the eccentricity variations induced by radiation pressure forces, described earlier. These account for removal of particles before collapse through Poynting–Robertson drag can accumulate since, as seen in (36), the eccentricity variations have the same period as the planet's orbital motion.

By a procedure similar to the above, we can examine the effect on the eccentricity of a circumplanetary particle due to the Poynting–Robertson force. The torque on the particle's orbit due to $\mathbf{F}_{P-R}$ is $m\dot{\mathbf{H}} = \mathbf{r} \times \mathbf{F}_{P-R}$. Expressing this in terms of the $\mathbf{a}$ and $\mathbf{b}$

vectors and integrating over ψ, ω, and Ω', as before, we find that $\dot{H}/H = \dot{a}/2a$. Expressing $\dot{e}$ in terms of $\dot{H}$ and $\dot{a}$ from (30a,b), we find that $\langle \dot{e} \rangle = 0$.

The orbital inclination can be shown to exhibit an oscillation with the orbital period of the planet (Shapiro, 1963). Therefore it is not of particular interest.

IX. DIFFERENTIAL DOPPLER EFFECT

Another, more subtle radiation drag, identified by McDonough (1975), operates because light emitted from the retreating eastern half of the Sun will be red-shifted, decreasing its momentum, while identical photons from the approaching western half will have increased momenta due to being blue-shifted. This asymmetric delivery of radiation momentum produces an additional transverse force on an interplanetary particle (Fig. 12).

We obtain a meaningful upper bound on the effect by considering half of the solar radiant energy to be emitted at the eastern limb and the remaining half at the western limb; that is, the particle (assumed on a circular orbit) no longer sees a spherical Sun but rather just two point sources, one slightly red-shifted and the other equally blue-shifted. The relative velocity between the particle and the eastern "light bulb" is

$$v_{rel} = \omega_\odot R_\odot - nr \sin \xi$$
$$= (\omega_\odot - n)r \sin \xi; \quad (56)$$

the orbital angular velocity of the particle is n, while the solar spin rate is $\omega_\odot$.

The transverse momentum resulting from two photons of rest momentum $p_0/2$, emitted on each side, striking the particle is then

$$P = (p_0/2)(1 + v_{rel}/c) \sin \xi$$
$$- (p_0/2)(1 - v_{rel}/c) \sin \xi$$
$$= p_0(v_{rel}/c) \sin \xi. \quad (57)$$

Following the radiation pressure derivation, and substituting for $\sin \xi$ and v_{rel}, we find

$$F_{DDE} = (Q_{pr}SA/c)(R_\odot^2/rc)(\omega_\odot - n). \quad (58)$$

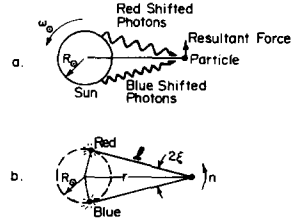This substantially overestimates the actual

FIG. 12. A schematic diagram of the differential Doppler effect. (a) Photons arriving at the particle from the retreating eastern hemisphere carry less momentum on the average (because of red-shifts) than do those from the approaching western hemisphere. The particle is pushed forward. (b) The Sun is modeled by point sources on each limb in order to use the relative velocity between the limb and the particle.

force since most solar energy comes from regions which have smaller Doppler shifts than the limb values; nevertheless the correction is less than an order of magnitude. The force is small and positive for distant particles but is a drag for particles within the synchronous orbit position.

If this force were larger than the Poynting–Robertson drag in certain regions, then particles could be driven inward when $F_{DDE} < F_{P-R}$ and outward when $F_{DDE} > F_{P-R}$ and large dust concentrations could accrue. However, from (17) and (58),

$$F_{DDE}/F_{P-R} = (R_\odot/r)^2[(\omega_\odot/n) - 1] \quad (59)$$

and thus the differential Doppler force is always less than the Poynting–Robertson drag. It is important only if a particle is near the solar surface (cf. Guess, 1962), where it adds to the Poynting–Robertson drag; however, it could be appreciable for particles orbiting a contact binary system (S. J. Weidenschilling, private communication, 1979). The effect is only significant because it provides a more profound insight into the phenomena that produce the Poynting–Robertson effect itself.

X. THE YARKOVSKY EFFECT

Elementary Considerations

We noted earlier that the transverse drag known as the Poynting–Robertson effect has been interpreted as caused by the aber-
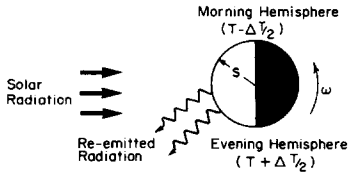
FIG. 13. The Yarkovsky effect. The evening hemisphere radiates extra energy and momentum because it is hotter than the morning hemisphere. For prograde rotation as shown, the particle is thrust forward the momentum carried away in the reemitted radiation.

ration from the radial direction of the *received* radiation. An angular displacement from the radial direction is also present in the *absorbed and reemitted* radiation any time a particle rotates and is not isothermal. The temperature pattern is skewed by the particle's rotation in concert with thermal lags; this can be viewed as an evening hemisphere that on the average is slightly warmer than the morning hemisphere, just as on planets. The warmer evening hemisphere radiates more energy, and hence momentum, than the cooler morning hemisphere. The reaction force due to the absorbed and reemitted radiation is found by integrating over the entire surface; in general the reaction force will have a transverse component analogous to the nongravitational forces which perturb cometary orbits (but, of course, the latter forces are produced by outgassing of volatiles rather than by emitting radiation; see Marsden, 1976; Whipple, 1978). Figure 13 depicts the essentials of this effect. One can anticipate that the force may involve the particle's rotation rate, thermal properties and dimensions, as well as the solar distance.

According to Öpik (1951), this process was first described around 1900 by an Eastern European civil engineer, I. O. Yarkovsky (for a biographical sketch, see Neiman *et al.*, 1965), in a pamphlet whose reference has been lost. The effect was twice independently rediscovered: by Radzievskii (1952) who, along with Öpik (1951), hinted at its dominance among perturbation effects for meter-sized particles, and again

by Peterson (1966) in his M.S. thesis. Our discussion will follow the physical arguments of Öpik (1951) but results will be compared against those of the more detailed treatment by Peterson (1976). Another recent analytical solution is presented by Hasegawa *et al.* (1977).

"Fast" Rotation vs "Slow" Rotation; "Large" Bodies vs "Small" Ones

The computation of the force will require a knowledge of the surface temperature on a rotating atmosphereless sphere of radius s having thermal diffusivity $\kappa = K/\rho C$, where ρ is mass density, K is thermal conductivity, and C is specific heat. At the outset we find it valuable to distinguish particles that are rotating rapidly from those spinning slowly, because the thermal distributions, both in the interior and on the surface, in the two cases are qualitatively different. A schematic diagram of the surface temperatures for the fast and slow cases is given as Fig. 14. The surface temperature of an element in sunlight is determined by a balance of the absorbed solar energy with the surface reemission plus that conducted to the interior. Starting on the left of the figure, at noon the temperature is at its peak and slowly decreases as the solar elevation drops, since in this region the surface layers are in equilibrium with the solar flux. Beginning at dusk the surface cools by
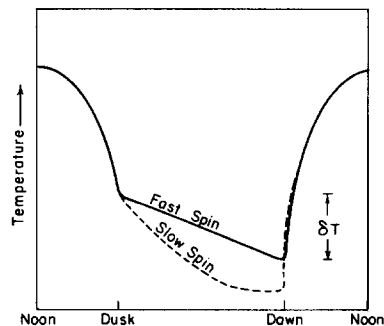

FIG. 14. Sketch of the surface temperature on a rotating body. Two cases are shown: The "fast" rotation (or "large" body) case is the solid line while the "slow" rotation (or "small" body) case is the dotted curve. See text.

radiation so that the interior conducts its warmer heat there. At fast spins the temperature decay at night is essentially linear as shown, the achieved δT being proportional to P. However, if the object rotates slowly enough, interior temperatures drop to the point where heat can be efficiently conducted through from the front; this causes the curve for slow spin to start to turn up near down; it would be symmetric for a nonrotating particle. Thus the maximum asymmetry on the night side will occur at spins near the transition between the slow and the fast rotation cases. Once dawn is reached, T grows quickly as equilibrium with the incoming radiation is sought. The morning surface temperature on rapidly spinning particles is cooler than with slow ones because in the fast case the temperature is not yet in equilibrium and appreciable heat is still being carried toward the center.

When an object falls into the rapid rotation class, its temperature fluctuations, as it turns in the sunlight, are restricted to surface layers, while in the slow spin case they penetrate deeply the particle's interior. We take the size dividing these cases to be

$$s = h, \qquad (60)$$

where h is the characteristic thickness traversed by a thermal pulse during half the rotation period $(P/2) = \pi/\omega$. To estimate h, we make use of the Green's function, which is the solution to a partial differential equation where a delta function is the source term. For the heat equation, the Green's function for the temperature T exhibits the characteristic manner in which T decays with time t and distance $\mathscr{S}$. Since the Green's function contains the term $e^{-\mathscr{S}^2/4\kappa t}$ (Greenberg, 1971, p. 67), the interior temperature is damped to e^{-1} the surface value at an approximate depth $\mathscr{S}$ of $2(\kappa t)^{1/2}$. Thus when considering the temperature fluctuations on a rotating particle, we are dealing only with a surface effect if the particle has a radius larger than the characteristic penetration depth of a thermal wave, i.e., if

$$s > (2\kappa P)^{1/2}; \qquad (61)$$

this is in agreement with the definition of a "large" body used by Öpik (1951) and Peterson (1976); see also Kaula (1968, p. 272). It should be remarked that the "large" body case is just as appropriately denoted the "fast" rotation case. Typical values for the material parameters of most silicates that form the surface layers of the Earth are $C = 10^7$ ergs $°K^{-1}g^{-1}$, $\rho = 2.5$ g cm^{-3}, $K = 3.5 \times 10^5$ ergs $°K^{-1}$ cm^{-1} sec^{-1} (Kaula, 1968; cf. Peterson, 1976). Then for stony bodies the criterion distinguishing surficial from total heating is

$$s \gtrsim 0.2\, P^{1/2}\ \text{cm}, \qquad (62a)$$

with P in seconds. For metal-rich objects, we choose $C = 5 \times 10^6$ ergs $°K^{-1}g^{-1}$, $\rho = 8.0$ g cm^{-3}, $K = 4 \times 10^6$ ergs $°K^{-1}$cm^{-1} sec^{-1}, in which case the criterion reads

$$s \gtrsim 0.5\, P^{1/2}\ \text{cm}. \qquad (62b)$$

If we take P to be the rotation period of the smallest observed asteroids $(D \gtrsim 1\ \text{km})$, all of which have periods in excess of several hours (Burns and Tedesco, 1979), (62) implies that objects larger than several tens of centimeters will fall into the "large" body case. Since, if anything, we expect interplanetary boulders to spin even faster than asteroids owing to the increased importance of collisions for smaller objects (cf. Öpik, 1951; Dohnanyi, 1976), we believe that all objects larger than 1 cm, or some number considerably smaller, will be "fast" rotators by our definition. If the surface layers of the particles are not solid but instead are rather porous or textured, as for a regolith, the right-hand sides of (62) are significant overestimates of the critical size. In this connection we note that the thermal inertias $(K\rho C)^{1/2}$ for the surfaces of the Galilean satellites and Phobos, according to eclipse radiometry (Morrison, 1977), are 2 or 3 orders of magnitude lower than those given by our choices of material parameters.

Temperature Changes on Rapidly Rotating Bodies

When the thermal effect is confined to the surface layers (i.e., $h < s$), the temperature change during a rotation may be estimated by equating the energy received with that stored in the volume contained in a thermal penetration depth h. During a complete rotation the energy striking an equatorial strip of unit height is $2sSP$. Thus for surface material with albedo δ the energy absorbed per rotation period by a unit area surface element on the equator is $(1 - \delta)SP/\pi$. The internal energy which is added to the thermal penetration layer during a temperature rise of ΔT is $\rho h C \Delta T \approx 2\Delta T(\pi K\rho C/\omega)^{1/2}$. Equating these, the typical temperature fluctuation within the thermal penetration depth for a rapidly rotating object is

$$\Delta T \approx (1 - \delta)\gamma S(P/2\pi)^{1/2}, \qquad (63)$$

where the inverse thermal inertia γ is $(K\rho C)^{-1/2}$ (Kaula, 1968). We will take this computed variation in the mean temperature of the layer to also measure the change in the surface temperature during a rotation. Our result is within 25% of Peterson's asymptotic value $(\Delta T/T \ll 1)$, which was found by solving the partial differential equation for the temperature variation on a cylinder's surface. Using the values for the parameters given previously, the temperature difference felt over the surface of a rapidly spinning stony body would be

$$\Delta T \approx \tfrac{1}{5} P^{1/2}/R^2, \qquad (64a)$$

which has the form of Öpik's (1951) result; his coefficient is $\tfrac{1}{6}$. However, we know neither the basis of his expression (beyond "dimensional analysis") nor his choice of parameters (beyond "proper values for stones"). For iron,

$$\Delta T \approx \tfrac{1}{25} P^{1/2}/R^2. \qquad (64b)$$

Yarkovsky Force for Rapid Rotation Case

The Yarkovsky force results from the fact, shown in Fig. 14, that the dusk-to-midnight portion radiates more than the midnight-to-dawn side while the dawn-to-noon area absorbs more radiation than does afternoon side. We idealize the actual temperature distribution by considering the entire evening hemisphere to be at a temperature $T + \Delta T/2$ whereas the morning hemisphere is at $T - \Delta T/2$, where ΔT is given by (63). For the force consider a surface element dA at temperature T, radiating isotropically into one hemisphere with intensity I; i.e., the entire surface is taken to radiate as a Lambert surface would. The outward energy flux is $\int I \cos \nu \, d\chi = \pi I = \sigma T^4$, where ν is the angle with respect to the surface normal, χ is solid angle, and σ is the Stefan–Boltzmann constant; we assume the surface emissivity $\epsilon(\lambda) \approx 1$. Then the radiation reaction upon the element, normal to its surface, is

$$dF = \int (I \cos \nu)(\cos \nu \, dA)d\chi/c$$
$$= \tfrac{2}{3} \sigma T^4 dA/c. \qquad (65)$$

For a spherical particle of radius s having the assumed surface temperature with $\Delta T/T \ll 1$, the transverse reaction force in the orbit plane—that is, the Yarkovsky force—resulting from the excess emission on the evening side is computed to be

$$F_Y = \tfrac{8}{3} \pi s^2 (\sigma T^4/c)(\Delta T/T) \cos \zeta; \qquad (66)$$

ζ is the particle's obliquity, the angle between its rotation axis and orbit pole. Note that this perturbation force can be either positive or negative, depending on whether the particle rotates prograde $(0 < \zeta < \pi/2)$ or retrograde $(\pi/2 < \zeta < \pi)$, respectively. If the rotation is retrograde, the particle's leading hemisphere has a larger force on it than the trailing side and so the Yarkovsky force then adds to the Poynting–Robertson drag, causing a faster inward spiral. However, for prograde rotation, as in Fig. 13, the Yarkovsky force opposes the Poynting–Robertson force and, if large enough, can actually produce outward spiraling.

In order to compare the Yarkovsky force to the Poynting–Robertson drag, we write

the latter from (5), assuming a circular orbit, as

$$F_{P-R} = -SAO_{pr}v/c^2. \qquad (67)$$

The ratio of (66) to (67) is then

$$F_Y/F_{P-R} \approx -\tfrac{2}{3}(c/v)(\Delta T/T)\cos\zeta. \quad (68)$$

Crudely, this can be viewed as the ratio of the asymmetry in the Yarkovsky problem ($\Delta T\cos\zeta/T$) to that of the Poynting–Robertson drag (v/c): the input energy has cancelled out because it is the same in the two cases. Since ($\Delta T/T$) is a function of orbital distance, as well as the composition and rotation period of a given particle (size being unimportant for these rapid rotators), while v varies with orbital position, it is possible that $F_Y = -F_{P-R}$ in parts of the inner solar system; for this to occur, $\Delta T/T$ need be merely of order 10^{-4}. In such regions, material could accumulate since particles are driven there, but not removed, by drag forces (see Gold, 1975).

The average surface temperature T is determined such that the absorbed energy flux, SAQ_{abs}, heats the sphere to the point that the reemitted energy flux, $4\pi s^2 \sigma T^4$, equals it. For macroscopic particles, $Q_{pr} \approx Q_{abs} \approx 1 - \delta$, ignoring any nonisotropic scattering. Hence the mean equilibrium temperature of a body in space is

$$T = [(S_0/R^2)(1 - \delta)/4\sigma]^{1/4}. \qquad (69)$$

This is approximate but only valid when $\Delta T/T$ is very small; otherwise significantly more energy appears in this formulation to be radiated away than is received. Defining $W = 2c(S_0^3\,\sigma)^{1/4}(r/R)^{1/2}/[3(\pi\,GM)^{1/2}] = 1.31 \times 10^7$ ergs AU sec^{-1} $^\circ$K^{-1}cm^{-2} and using (69) in (68) with (63), the Yarkovsky force relative to the Poynting–Robertson drag is

$$F_Y/F_{P-R}$$
$$= -W\gamma(1 - \delta)^{3/4}P^{1/2}\cos\zeta/R \quad (70)$$

for rapidly spinning particles. This will be considered again following the next section.

The maximum value of the Yarkovsky force for the fast case will occur when ΔT becomes as large as possible; as can be seen from Fig. 14, this will also be the largest possible force for all situations, since at slower rotation rates, conduction of heat starts to equalize the surface temperatures on the two sides of the noon–midnight line. The maximum Yarkovsky force then is from (68)

$$F_Y/F_{P-R}|_{max}$$
$$= -W(1 - \delta)^{3/4}s\cos\zeta/2^{1/2}KR, \quad (71)$$

where ΔT has taken its value at the transition from "slow" to "fast" rotation. For stony objects this is about $20s/R$, where s is in centimeters and R in astronomical units; for irons it is about an order of magnitude less.

Yarkovsky Force for "Slowly" Rotating Bodies

In the slow rotation case the temperature on the night side at the start drops linearly with time. In this region Eq. (63) will represent ΔT if the rotation period P there is replaced by the thermal penetration time $\tau = s^2/2\kappa$ from (61); this decreases the effect over what it would be if the fast spin condition were still satisfied. The Yarkovsky force is further reduced due to the shifted location of the asymmetry in the reradiation and the absorption; as slower and slower rotations are considered, the radiation and absorption patterns become more and more symmetrical with respect to the direction along which the radiation arrives. We account for this feature by multiplying the Yarkovsky force by τ/P, which gives the correct result in the limits $P \approx \tau$ and $P \to \infty$; Öpik (1951) does not include this factor. With these modifications, we find from (63), (68), and (69)

$$F_Y/F_{P-R} = -W(1 - \delta)^{3/4}s^3\cos\zeta/$$
$$[P(2)^{3/2}RK\kappa] \quad (72)$$

for slowly rotating objects. For this case Öpik (1951) found $F_Y/F_{P-R} \sim s\cos\zeta/R$, a result like (71) while a linearization of Peterson (1976) for small P has the force ratio $\sim\cos\zeta/RP^{1/2}$. Our disagreements are

not too important for, as we shall see, the fast rotation case is more probable.

The Probable Yarkovsky Force

It is beyond the scope of this paper to calculate probable rotation rates. Nevertheless, as mentioned earlier, most likely the heating is a skin effect (cf. Öpik, 1951; Hasegawa *et al.*, 1977) because small interplanetary bodies are believed to rotate very rapidly, owing either to collisions with other small bodies (McAdoo and Burns, 1973; Burns, 1975; Harris and Burns, 1979; Burns and Tedesco, 1979; Öpik, 1951; Dohnanyi, 1971, 1972, 1976b; Harris, 1979) or differential radiation forces (Radzievskii, 1954; Paddack, 1969; Paddack and Rhee, 1976; Icke, 1973). The potential of each of these processes to produce rapid spins is easily understood. In the first case a colliding cloud of bodies will, when in "thermal" equilibrium, distribute its kinetic energy equally between the random velocity components (i.e., the noncircular part of the orbital velocity) and the intrinsic spins of the objects making up the cloud; enormous rotational velocities are so produced unless a drag is present or equilibrium has not been reached. Radiation forces may also be very effective in spinning up small particles: according to the discussion following (45), such particles during their lifetimes are struck by amounts of radiation whose equivalent mass may exceed the particle mass. This radiation impacts the particle at velocity c and, hence, if there is the slightest systematic asymmetry in the way it is absorbed or reflected, it is capable of delivering huge amounts of angular momentum: as a result the particles will spin very fast. Larger particles are not as affected by these processes and therefore rotate more slowly, but they probably still have thermal penetration depths much less than their radii. Thus we expect that (70) is more appropriate to use for estimating the Yarkovsky perturbation than is (72).

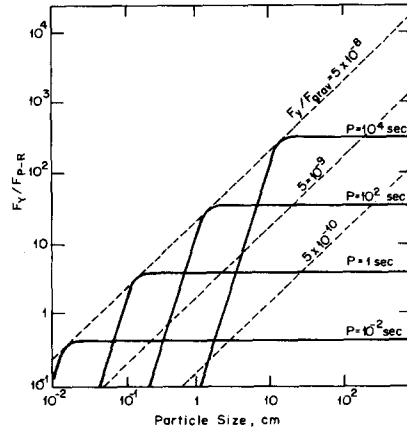We show in Fig. 15 the ratio of the Yarkovsky force to the Poynting–Robertson

FIG. 15. The ratio of the Yarkovsky force to the Poynting–Robertson drag for various spin periods and particle sizes for stony particles at 1 AU. The top dotted line depicts the transition from the fast rotation case to the slow spin case and gives the maximum Yarkovsky force; the numbers on the sloping dotted lines are the ratio of the Yarkovsky perturbation to gravity.

drag for stony objects at 1 AU; for irons the fast spin curves would be reduced by a factor of about 4 while their slow spin curves would be down by nearly 100. The level lines on the right-hand portion are the solution (70) for fast rotations whereas the left-hand curves, having a slope of $+3$ for small s, are for slow spins (Eq. 72). The transition between these two cases comes from (71); as shown, it also forms the envelope of the family of solution curves for various spin rates; for irons it would be shifted to the right by log 2.5. We notice that for most objects larger than dust grains the *Yarkovsky force dominates the Poynting–Robertson drag;* nevertheless, since the latter has constant direction whereas the former's sign depends on the spin direction, the Poynting–Robertson drag may dominate over long evolution times.

We remind the reader that the strength of the perturbation due to the Yarkovsky force is found by comparison against the gravitational attraction. It is in this sense that (71) gives the maximum force. The Yarkovsky perturbation relative to gravity at the critical size is $F_Y/F_{grav}|_{max} = \beta(F_{P-R}/F_{RP})$ (F_Y/F_{P-R}) or $(20s/R)(v/c)\beta$ for stones.

Using (71) and considering objects for which geometrical optics holds, $F_Y/F_{grav}|_{max} \approx 5 \times 10^{-8}R^{-3/2}$, a very small perturbation but one that over 10^7–10^8 years will cause complete orbital collapse if the object has a continuous retrograde spin. The relative perturbation for spin rates other than the critical one are found by scaling and are shown dotted in Fig. 15.

The dynamics resulting from Yarkovsky forces are quite complicated (Dohnanyi, 1978). The orbital evolution produced is described by a random walk process of varying step size and direction. This occurs because collisions, being statistical vector additions of angular momentum, are as likely to produce prograde as retrograde rotations if much angular momentum is transferred in such a manner (Burns and Safronov, 1973; Harris, 1979). Thus perturbation forces occur in random directions and orbits may spiral erratically inward or outward (the latter provided $F_Y/F_{P-R} > 1$). Moreover, Slabinski (1977) even questions whether the Yarkovsky force will have a cumulative effect on objects less than a meter in size; he points out that solar radiation pressure will produce precession of the spin axis and thereby will cause the Yarkovsky force to average to zero over long times. The random orientation of the particle's angular velocity vector also means that orbital inclinations will evolve.

It is important to note that the Yarkovsky force depends upon the body's composition [see (70) and (72)], such that the maximum perturbation on a stony object is ten times that on an iron. Thus the orbital evolution timescales may differ for stony and iron objects. In this regard, Peterson (1976) has suggested that the markedly younger cosmic-ray exposure ages for stony versus iron meteorites are produced by the more rapid orbital evolution of the stones under the Yarkovsky effect as seen by substituting (64a) and (64b) in (68). He believes that meteorites are delivered to the Earth in a two-stage process following their production in asteroidal collisions: changes in the orbit size caused by the Yarkovsky effect permit secular resonances with Jupiter to be achieved and then secular responses allow rapid modification into Earth-crossing orbits.

XI. SUMMARY

We have derived in two original ways the radiation pressure force and Poynting–Robertson drag on small particles in the solar system; our derivations include the first accurate, general treatment of the role of scattering in addition to absorption of sunlight. In order to investigate interplanetary dust, we have used Mie calculations, employing actual optical properties and the solar spectrum, to compute radiation pressure efficiency factors, to which both forces are proportional. We have found the forces felt by 0.005- to 10.0-μm particles composed of water ice, graphite, iron, magnetite, basalt, amorphous quartz, and obsidian. These results show that only for iron, magnetite, and graphite does the radiation pressure force exceed gravity and, even then, just for a fairly narrow size range. This implies that only particles of quite specific sizes and composition can be easily ejected from the solar system. Objects of larger sizes are lost by collapse of their orbits under Poynting–Robertson drag; smaller sizes are eliminated by solar wind drag. Although not calculated, it appears as though destruction by collisions or sublimation may be more important loss mechanisms. We have briefly reviewed the circumstances under which material can be ejected, and how orbits evolve with these perturbations as well as with changes in particle sizes. We have also described how the orbits of small particles moving about planets are modified by these radiation forces.

We have presented physical arguments to approximately derive two other forces resulting from solar radiation. One, recently discovered by McDonough (1975), is produced by the different signs of the Doppler shifts for the radiation from the two solar

hemispheres. We have found that this force is always less than the Poynting–Robertson force and that its sign depends on whether or not its orbit lies within the solar synchronous orbit. We have also derived the Yarkovsky force in a manner more complete than the original English language presentation of Öpik (1951) and more accessible than the detailed analytical treatment of Peterson (1976). This force arises owing to asymmetric absorption and reradiation of the received solar energy for a rotating body having thermal lags. The Yarkovsky effect, depending on material properties, dominates other dissipative perturbations for bodies that are meters in size.

The derivations of the four effects presented above have clarified and, in some cases, generalized previous developments. This should permit a better and broader understanding of some of the important forces that modify the orbits of small objects in the solar system. Nevertheless the problem of determining the orbital evolution of interplanetary particles is far from resolved. New approaches are necessary for calculating the long-term effects of planetary perturbations, stochastic collisions, and electromagnetic forces, each of which may itself be of overriding significance for certain particles. Until these problems are solved, the life history of a typical member of the interplanetary complex will remain obscure.

APPENDIX: NOMENCLATURE

a	Semimajor axis
$\mathbf{a}$	Vector along line of apses in direction of pericenter (see Fig. 9)
A	Area
Å	Angstrom
b	Semiminor axis
$\mathbf{b}$	Vector along semiminor axis (see Fig. 9)
c	Speed of light; projectile speed
$\hat{\mathbf{c}}$	Unit vector equaling $\hat{\mathbf{a}} \times \hat{\mathbf{b}}$ (see Fig. 9)
C	Specific heat
C_{D}	Drag coefficient
d	Refractive index
e	Eccentricity
E	Orbital energy, energy flux
E_{i}	Incoming energy flux
f	True anomaly; absorption fraction
$f(\alpha)$	Scattering phase function
$\mathbf{F}$	Force
F_i	Force component in i direction
$(F_{\text{R}}, F_{\text{T}}, F_{\text{N}})$	Radial, transverse, normal components of force vector
g	Scattered fraction
G	Universal gravitational constant
h	$(e/Z) \sin \tilde{\omega}$,
$\mathcal{K}$	thermal penetration depth
H	Orbital angular momentum per unit mass
i	Inclination; $\sqrt{-1}$
I	Radiation intensity
k	$(e/Z) \cos \tilde{\omega}$
K	Thermal conductivity
l	Path length for differential Doppler effect
L	Solar luminosity
m	Particle mass
M	Solar mass; projectile mass
$\mathcal{M}$	Mean anomaly
n	Mean motion of particle
p	Momentum flux
pr	Pressure
P–R	Poynting–Robertson
P	Rotation period
P_{o}	Orbital period
$Q_{\text{pr}}, Q_{\text{abs}}, Q_{\text{sca}}$	Mie scattering coefficients
r	Radius to particle
r_{o}	Earth's orbital radius
$\hat{\mathbf{r}}$	Radial unit vector
R	Orbital radius in AU; solar radius
s	Particle radius
S	Solar energy flux density
S'	Doppler-shifted solar energy flux density
S_{o}	Solar constant

$\hat{S}$	Unit vector in direction of beam
t	Time
t_{P-R}	Collapse time under Poynting–Robertson Drag
T	Temperature
u	Velocity parallel to beam
v	Velocity perpendicular to beam; velocity along particle path
Δv	Velocity increment along beam
(x,y,z)	Coordinates
W	Coefficient of (70)
X	Mie scattering parameter $= 2\pi s/\lambda$
Z	$\frac{3}{2}[a(1 - e^2)/\mu]^{1/2}\, F/mn$
α	Scattering angle (see Fig. 3)
β	F_R/F_g, force ratio (19)
γ	$(1 - v^2/c^2)^{-1/2}$; inverse thermal inertia
δ	Albedo
ϵ	Emissivity
ζ	Obliquity
η	Coefficient in (47)
θ	Orbital longitude
$\hat{\theta}$	Transverse unit vector
κ	Thermal diffusivity
λ	Wavelength; mean longitude of Sun $= n_\odot t$
μ	GM
μ'	$GM\,(1 - \beta)$
$\mu\mathrm{m}$	Micron
ν	Angle relative to normal
ξ	Half-angle of Sun (see Fig. 10); trajectory angle (see Fig. 4)
$\tilde{\omega}$	$\omega + \Omega$, longitude of pericenter
ρ	Particle density
σ	Stefan–Boltzmann constant
τ	$\int_0^{P_0/2} \hat{b} \cdot \hat{S}\, dt$; thermal penetration time
χ	Solid angle annulus
ψ	Eccentric anomaly

Ω	Solar solid angle, longitude of node
Ω'	Longitute of node with respect to subsolar direction $= \Omega\text{-}n_\odot t$
$\Omega_\odot$	Solar spin rate
ω	Spin rate; argument of pericenter

ACKNOWLEDGMENTS

REFERENCES

AANNESTAD, P. A., AND PURCELL, E. M. (1973). Interstellar grains. *Ann. Rev. Astron. Astrophys.* 11, 309–362.

ALLEN, R. R. (1961). Satellite orbit perturbations in vector form. *Nature* 190, 615.

ALLAN, R. R. (1962). Satellite orbit perturbations due to radiation pressure and luni-solar forces. *Quart. J. Mech. Appl. Math.* 15, 281–301.

ALLAN, R. R. (1967). Resonance effects due to the longitude dependence of the gravitational field of a rotating primary. *Planet. Space Sci.* 15, 53–76.

ARVESEN, J. C., GRIFFIN, R. N., JR., AND PEARSON, B. D., JR. (1969). Determination of extraterrestrial solar spectral irradiance from a research aircraft. *Appl. Opt.* 8, 2215–2232.

ASHWORTH, D. G. (1978). Lunar and planetary impact erosion. In *Cosmic Dust* (J. A. M. McDonnell, Ed.), pp. 427–526. Wiley, Chichester.

BEARD, D. B. (1963). Comets and cometary debris in the solar system. *Rev. Geophys.* 1, 211–229.

BELTON, M. J. S. (1966). Dynamics of interplanetary dust. *Science* 151, 35–44.

BERG, O. E., AND GRÜN, E. (1973). Evidence of hyperbolic cosmic dust particles. *Space Res.* 13, 1047–1055.

BERTAUX, J. L., AND BLAMONT, J. E. (1973). Interpretation of OGO 5 Lyman alpha measurements in the upper geocorona. *J. Geophys. Res.* 78, 80–91.

BERTAUX, J. L., AND BLAMONT, J. E. (1976). Possible

evidence for penetration of interstellar dust into the solar system. *Nature* **262**, 263–266.

BERTIE, J. E., LABBÉ, H. J., AND WHALLEY, E. (1969). Absorptivity of ice I in the range 4000–30 cm⁻¹. *J. Chem. Phys.* **50**, 4501–4520.

BEST, G. T., AND PATTERSON, T. N. L. (1962). The capture of small absorbing particles by the solar radiation field. *Planet. Space Sci.* **9**, 801–809.

BIBRING, J. P., LANGEVIN, Y., MAURETTE, M., MEUNIER, R., JOUFFREY, B., AND JOURET, C. (1974). Ion implantation effects in "cosmic" dust grains. *Earth Planet. Sci. Lett.* **22**, 205–214.

BROWN, R. A., AND YUNG. Y. L. (1976). Io, its atmosphere and optical emissions. In *Jupiter* (T. Gehrels, Ed.), pp. 1102–1145. Univ. of Arizona Press, Tucson.

BROWNLEE, D. E. (1978a). Interplanetary dust: Possible implications for comets and pre-solar interstellar grains. In *Protostars and Planets* (T. Gehrels, Ed.), pp. 134–150. Univ. of Arizona Press, Tucson.

BROWNLEE, D. E. (1978b). Microparticle studies by sampling techniques. In *Cosmic Dust* (J. A. M. McDonnell, Ed.), pp. 295–336. Wiley, Chichester.

BROWNLEE, D. E., AND RAJAN, R. S. (1973). Micrometeorite craters discovered on chondrule-like objects from Kapoeta meteorite. *Science* **182**, 1341–1344.

BROWNLEE, D. E., HÖRZ, F., VEDDER, J. F., GAULT, D. E., AND HARTUNG, J. B. (1973). Some physical parameters of micrometeoroids. *Proc. 4th Lunar Sci. Conf.*, **3**, 3197–3212.

BROWNLEE, D. E., HÖRZ, F., HARTUNG, J. B., AND GAULT, D. E. (1975). Density, chemistry and size distribution of interplanetary dust. *Proc. 6th Lunar Sci. Conf.* **3**, 3409–3416.

BROWNLEE, D. E., HÖRZ, F., TOMANDL, D. A., AND HODGE, P. W. (1976). Physical properties of interplanetary grains. In *The Study of Comets* (B. Donn, M. Mumma, W. Jackson, M. A'Hearn, and R. Harrington, Eds.), Part 2, pp. 962–982. NASA SP-393.

BROWNLEE, D. E., TOMANDL, D. A., AND OLSZEWSKI, E. (1977). Interplanetary dust; a new source of extraterrestrial material for laboratory studies. *Proc. 8th Lunar Sci. Conf.* **1** 149–160.

BRYANT, R. W. (1961). Effect of solar radiation pressure on the motion of an artificial satellite. *Astron. J.* **66**, 430–432.

BURNS, J. A. (1975). The angular momenta of solar system bodies: Implications for asteroid strengths. *Icarus* **25**, 545–554.

BURNS, J. A. (1976). An elementary derivation of the perturbation equations of celestial mechanics. *Amer. J. Phys.* **44**, 944–949. See *Amer. J. Phys.* **45**, 1230.

BURNS, J. A. (1977). Orbital evolution. In *Planetary Satellites* (J. A. Burns, Ed.), pp. 113–156. Univ. of Arizona Press, Tucson.

BURNS, J. A., AND SAFRONOV, V. S. (1973). Asteroid nutation angles. *Mon. Not. Roy. Astron. Soc.* **165**, 403–411.

BURNS, J. A., AND SOTER, S. (1979). Radiation pressure and Poynting–Robertson drag on scattering particles: A new, simple derivation. In *Solid Particles in the Solar System*, IAU Symp. 90, Ottawa, Canada.

BURNS, J. A., AND TEDESCO, E. F. (1979). Asteroid brightness variations: Implications for rotation rates and shapes. In *Asteroids* (T. Gehrels, Ed.). Univ. of Arizona Press, Tucson.

CHAMBERLAIN, J. W. (1979). Depletion of satellite atoms in a collisionless exosphere by radiation pressure. *Icarus* **39**, 286–294.

CHERNYAK, Y. B. (1978). On recent lunar atmosphere. *Nature* **273**, 497–501.

CONSOLMAGNO, G. J. (1978). *Electromagnetic Processes in the Evolution of the Solar Nebula*, Ph.D. thesis, University of Arizona; see *Icarus* **38**, 398–410.

CONSOLMAGNO, G., AND JOKIPII, J. R. (1977). Lorentz scattering of interplanetary dust. *Bull. Amer. Astron. Soc.* **9**, 519–520.

CRUIKSHANK, D. P. (1979). The satellites of Saturn: A pre-encounter review. *Rev. Geophys. Space Phys.* **17**, 165–176.

CUZZI, J. N., AND POLLACK, J. B. (1978). Saturn's rings: Particle composition and size distribution as constrained by microwave observations. I. Radar observations. *Icarus* **33**, 233–262.

DANBY, J. M. A. (1962). *Fundamentals of Celestial Mechanics*. Macmillan Co., New York.

DAY, K. L. (1977). Interstellar silicates. *Astron. Quart.* **1**, 21–36.

DELSEMME, A. H. (1976). Can comets be the only source of interplanetary dust? In *Interplanetary Dust and Zodiacal Light* (H. Elsässer and H. Fechtig, Eds.), pp. 481–484. Springer-Verlag, Berlin.

DIVARI, N. B., AND REZNOVA, L. V. (1970). Stellar radiation pressure upon spherical interstellar particles. *Sov. Astron.-AJ* **14**, 133–138.

DOBROVOL'SKII, O. V., EGIBEKOV, P., AND ZAUSAEV, A. F. (1974). Nongravitational effects on the evolution of dust particles moving in elliptical orbits about the Sun. *Sov. Astron.-AJ* **17**, 527–528.

DOHNANYI, J. (1971). Fragmentation and distribution of asteroids. In *Physical Studies of Minor Planets* (T. Gehrels, Ed.), pp. 263–295. NASA SP-267.

DOHNANYI, J. S. (1972). Interplanetary objects in review: Statistics of their masses and dynamics. *Icarus* **17**, 1–48.

DOHNANYI, J. S. (1976a). Flux of hyperbolic meteoroids. In *Interplanetary Dust and Zodiacal Light* (H. Elsässer and H. Fechtig, Eds.), pp. 170–180. Springer-Verlag, Berlin.

DOHNANYI, J. S. (1976b). Sources of interplanetary dust: Asteroids. In *Interplanetary Dust and*

Zodiacal Light (H. Elsässer and H. Fechtig, Eds.), pp. 187–205. Springer-Verlag, Berlin.

DOHNANYI, J. S., (1978). Particle dynamics. In *Cosmic Dust* (J. A. M. McDonnell, Ed.), pp. 527–605. Wiley, Chichester.

DONNISON, J. R., AND WILLIAMS, I. P. (1977a). The effects of a resisting medium on protoplanetary orbits. *Mon. Not. Roy. Astron. Soc.* **180**, 281–288.

DONNISON, J. R., AND WILLIAMS, I. P. (1977b). The resistive effect of the solar wind on the orbits of solid bodies in the solar system. *Mon. Not. Roy. Astron. Soc.* **180**, 289–296.

DORSCHNER, J. (1971). Dust production in circumstellar space. *Astron. Nachr.* **293**, 65–70.

DRUMMOND, D. G. (1935). The infra-red absorption spectra of quartz and fused silica from 1 to 7.5 μ. II. Experimental results. *Proc. Roy. Soc. Ser. A* **153**, 328–339.

DUENNEBIER, F. K., NAKAMURA, Y., LATHAM, G. V., AND DORMAN, H. J. (1976). Meteoroid storms detected on the Moon. *Science* **192**, 1000–1002.

DUMONT, R. (1976). Ground-based observations of the zodiacal light. In *Interplanetary Dust and Zodiacal Light* (H. Elsässer and H. Fechtig, Eds.), pp. 85–100. Springer-Verlag, Berlin.

EINSTEIN, A. (1905). Zur Electrodynamik bewegter Körper. *Ann. Phys. (Leipzig)* **17**. English translation (On the electrodynamics of moving bodies) in *The Principle of Relativity*, pp. 35–65. Dover, New York.

FANG, T.-M. (1976). The spatial distribution of long-lived gas clouds emitted by satellites in the outer solar system. *Planet. Space Sci.* **24**, 577–588.

FECHTIG, H. (1976). In-situ records of interplanetary dust particles-methods and results. In *Interplanetary Dust and Zodiacal Light* (H. Elsässer and H. Fechtig, Eds.), pp. 143–158. Springer-Verlag, Berlin.

FECHTIG, H., GRÜN, E. AND KISSEL, J. (1978). Laboratory simulation. In *Cosmic Dust* (J. A. M. McDonnell, Ed.), pp. 607–669. Wiley, Chichester.

FINSON, M. L., AND PROBSTEIN, R. F. (1968a). A theory of dust comets. I. Model and equations. *Astrophys. J.* **154**, 327–352.

FINSON, M. L., AND PROBSTEIN, R. F. (1968b). A theory of dust comets. II. Results for comet Arend–Roland. *Astrophys. J.* **154**, 353–380.

FRIED, J. W. (1978). Doppler shifts in the zodiacal light spectrum. *Astron. Astrophys.* **68**, 259–264.

GANAPATHY, R., BROWNLEE D. E., AND HODGE, P. W. (1978). Silicate spherules from deep-sea sediments: Confirmation of extraterrestrial origin. *Science* **201**, 1119–1121.

GIESE, R. H. (1977). Interpretation of the optical properties of interplanetary dust. *J. Geophys.* **42**, 705–716.

GIESE, R. H. AND GRÜN, E. (1976). The compatibility of recent micrometeoroid flux curves with observations and models of the zodiacal light. In *Interplanetary Dust and Zodiacal Light* (H. Elsässer and H. Fechtig, Eds.), pp. 135–139. Springer-Verlag, Berlin.

GIESE, R. H., WEISS, K., ZERULL, R. H., AND ONO, T. (1978). Large fluffy particles: A possible explanation of the optical properties of interplanetary dust. *Astron. Astrophys.* **65**, 265–272.

GINDILIS, L. M., DIVARI, N. B., AND REZNOVA, L. Y. (1969). Solar radiation pressure of interplanetary dust. *Soviet Astron.-AJ* **13**, 114–119.

GOLD, T. (1975). Resonant orbits of grains and the formation of satellites. *Icarus* **25**, 489–491.

GOLDREICH, P., AND TREMAINE, S. (1979). Towards a theory for the uranian rings. *Nature* **227**, 97–99.

GORBAN, N. Y., STASHCHUCK, V. S., SHIRIN, A. V., AND SHISHLOVSKII, A. A. (1973). Optical properties of nickel–iron alloys in the region of interband transitions. *Opt. Spectrosc.* **35**, 295–298.

GOSWAMI, J. N., HUTCHEON, I. E., AND MACDOUGALL, J. D. (1976). Microcraters and solar flare tracks in crystals from carbonaceous chondrites and lunar breccias. *Proc. 7th Lunar Sci. Conf.* **1**, 543–562.

GRARD, R. J. L., ED. (1973). *Photon and Particle Interactions with Surfaces in Space.* Reidel, Dordrecht.

GREENBERG, J. M. (1978). Interstellar dust. In *Cosmic Dust* (J. A. M. McDonnell, Ed.), pp. 187–294. Wiley, Chichester.

GREENBERG, M. D. (1971). *Application of Green's Functions in Science and Engineering.* Prentice-Hall, Englewood Cliffs, N.J.

GRÜN, E., FECHTIG, H., KISSEL, J., AND GAMMLEIN, P. (1977). Micrometeoroid data from the first two orbits of Helios 1. *J. Geophys.* **42**, 717–726.

GUESS, A. W. (1962). Poynting–Robertson effect for a spherical source of radiation. *Astrophys. J.* **135**, 855–866.

HÄMEEN-ANTTILA, K. (1962). *Ann. Acad. Scient. Fenn.* **AVI**, 112.

HANSEN, J. E., AND TRAVIS, L. D. (1974). Light scattering in planetary atmospheres. *Space Sci. Rev.* **16**, 527–610.

HARRIS, A. W. (1979). Asteroid rotation. II. A theory for the collisional evolution of rotation rates. *Icarus* **40**, 145–153.

HARRIS, A. W., AND BURNS, J. A. (1979). Asteroid rotation. I. Tabulation and analysis of rates, pole positions, and shapes. *Icarus*, **40**, 115–144.

HARTUNG, J. B. (1976). Lunar microcraters and interplanetary dust fluxes. In *Interplanetary Dust and Zodiacal Light* (H. Elsässer and H. Fechtig, Eds.), pp. 209–226. Springer-Verlag, Berlin.

HARTUNG, J. B., HODGES, F., HÖRZ, F., AND

STORZER, D. (1975). Microcrater investigations on lunar rock 12002. *Proc. 6th Lunar Sci. Conf.* **3**, 3351–3371.

HARWIT, M. (1963). Origins of the zodiacal dust cloud. *J. Geophys. Res.* **68**, 2171–2180.

HARWIT, M. (1973). *Astrophysical Concepts.* Wiley, New York.

HASEGAWA, H., FUJIWARA, A., KOIKE, C., AND MUKAI, T. (1977). Effect of spin of an interplanetary dust on its motion. *Mem. Faculty Sci. Kyoto U. Ser. A* **35**, 131–139.

HEATH, D. F., AND SACHER, P. A. (1966). Effects of a simulated high-energy space environment on the ultraviolet transmittance of optical materials between 1050 Å and 3000 Å. *Appl. Opt.* **5**, 937–943.

HEMENWAY, C. L. (1976). Submicron particles from the Sun. In *Interplanetary Dust and Zodiacal Light* (H. Elsässer and H. Fechtig, Eds.), pp. 251–269. Springer-Verlag, Berlin.

HERRICK, S. (1948). A modification of the "variation-of-constants" method for special perturbations. *Publ. Astron. Soc. Pacific* **60**, 321–323.

HÖRZ, F., HARTUNG, J. B., AND GAULT, D. E. (1971). Micrometeorite craters on lunar rock surfaces. *J. Geophys. Res.* **76**, 5770–5798.

HÖRZ, F., BROWNLEE, D. E., FECHTIG, H., HARTUNG, J. B., MORRISON, D. A., NEUKUM, G., SCHNEIDER, E., VEDDER, J. F., AND GAULT D. E. (1975). Lunar microcraters: Implications for the micrometeroid complex. *Planet. Space Sci.* **23**, 151–172.

HOYLE, F., AND WICKRAMASINGHE, N. C. (1977). Origin and nature of carbonaceous material in the galaxy. *Nature* **270**, 701–703.

HUFFMAN, D. R. (1977). Interstellar grains: The interaction of light with a small particle system. *Advan. Phys.* **26**, 129–230.

HUFFMAN, D. R., AND STAPP, J. L. (1973). Optical measurements on solids of possible interstellar importance. In *Interstellar Dust and Related Topics* (J. M. Greenberg and H. C. van der Hulst, Eds.), pp. 297–301. Reidel, Dordrecht.

HUGHES, D. W. (1978). Meteors. In *Cosmic Dust* (J. A. M. McDonnell, Ed.), pp. 123–185. Wiley, Chichester.

HUTCHEON, I. D. (1975). Micrometeorites and solar flare particles in and out of the ecliptic. *J. Geophys. Res.* **80**, 4471–4483.

ICKE, V. (1973). Distribution of the angular velocities of the asteroids. *Astron. Astrophys.* **28**, 441–445.

JACKSON, J. D. (1962). *Classical Electrodynamics.* Wiley, New York.

KAULA, W. M. (1968). *An Introduction to Planetary Physics.* Wiley, New York.

KNACKE, R. F. (1977). Carbonaceous compounds in interstellar dust. *Nature* **269**, 132–134.

KRESÁK, L'. (1976). Orbital evolution of the dust streams released from comets. *Bull. Astron. Inst. Czech.* **27**, 35–46.

KRESÁK, L'. (1978). The mass distribution and sources of interplanetary boulders. *Bull. Astron. Inst. Czech.* **29**, 135–149.

LAMY, P. L. (1974a). The dynamics of circumsolar dust grains. *Astron. Astrophys.* **33**, 191–194.

LAMY, P. L. (1974b). Interaction of interplanetary dust grains with the solar radiation field. *Astron. Astrophys.* **35**, 197–207.

LAMY, P. L. (1975). *On the Dynamics of Interplanetary Dust Grains.* Ph.D. thesis, Cornell University.

LAMY, P. L. (1976). Orbital evolution of circumsolar dust grains. In *Interplanetary Dust and Zodiacal Light* (H. Elsässer and H. Fechtig, Eds.), pp. 437–442. Springer-Verlag, Berlin.

LAMY, P. L. (1978). Optical properties of silicates in the far ultraviolet. *Icarus,* **34**, 68–75.

LAMY, P. L., AND JOUSSELME, M. F. (1976). Temperature distribution and lifetime of interplanetary ice grains. In *Interplanetary Dust and Zodiacal Light* (H. Elsässer and H. Fechtig, Eds.), pp. 443–447. Springer-Verlag, Berlin.

LEINERT, C. (1975). Zodiacal light—a measure of the interplanetary environment. *Space Sci. Rev.* **18**, 281–339.

LEINERT, C., LINK, H., PITZ, E., AND GIESE, R. H. (1976). Interpretation of a rocket photometry of the inner zodiacal light. *Astron. Astrophys.* **47**, 221–230.

LENHAM, A. P., AND TREHERNE, D. M. (1966a). The optical properties of the transition metals. In *Optical Properties and Electronic Structures of Metals and Alloys* (F. Abélès, Ed.), pp. 196–201. North Holland, Amsterdam.

LENHAM, A. P., AND TREHERNE, D. M. (1966b). Optical constants of transition metals in the infrared. *J. Opt. Soc. Amer.* **56**, 1137–1138.

LESERGEANT, L. B., AND LAMY, P. L. (1978). Interplanetary dust: Are there two independent populations? *Nature* **276**, 800–802.

LESERGEANT, L. B., AND LAMY, P. L. (1979). On the size distribution and physical properties of interplanetary dust grains. Submitted to *Icarus.*

LEVY, E. H., AND JOKIPII, J. R. (1976). Penetration of interstellar dust into the solar system. *Nature* **264**, 423–424.

LIDOV, M. L. (1969). Secular effects in the evolution of orbits under the influence of radiation pressure. *Cosmic Res.* **7**, 423–436.

LILLIE, C. F. (1976). The ultraviolet scattering efficiency of interplanetary dust grains. In *Interplanetary Dust and Zodiacal Light* (H. Elsässer and H. Fechtig, Eds.), p. 63. Springer-Verlag, Berlin.

LUMME, K. (1972). On the formation of Saturn's rings. *Astrophys. Space Sci.* **15**, 404–415.

LYTTLETON, R. A. (1976). Effects of solar radiation on

the orbits of small particles. *Astrophys. Space Sci.* **44**, 119–140.

MAKAROVA, YE. A., AND KHARITONOV, A. V. (1972). *Distribution of Energy in the Solar Spectrum and the Solar Constant.* Nauka Moscow (NASA TT F-803).

MALITSON, I. H. (1965). Interspecimen comparison of the refractive index of fused silica. *J. Opt. Soc. Amer.* **55**, 1205–1209.

MANDEVILLE, J.-C. (1977). Impact microcraters on 12054 rock. *Proc. 8th Lunar Sci. Conf.,* 883–888.

MANDEVILLE, J.-C., AND VEDDER, J. F. (1971). Microcraters formed in glass by low density projectiles. *Earth Planet. Sci. Lett.* **11**, 297–306.

MARGOLIS, S. H., AND SCHRAMM, D. N. (1977). Dust in the universe? *Astrophys. J.* **214**, 339–346.

MARSDEN, B. G. (1974). Comets. *Ann. Rev. Astron. Astrophys.* **12**, 1–21.

MARSDEN, B. G. (1976). Nongravitational forces on comets. In *The Study of Comets* (B. Donn, M. Mumma, W. Jackson, M. A'Hearn and R. Harrington, Eds.), pp. 465–489. NASA SP-393.

MARTIN, P. G. (1978). *Cosmic Dust.* Oxford Univ. Press, Oxford.

MCADOO, D. C., AND BURNS, J. A. (1973). Further evidence for collisions among asteroids. *Icarus* **18**, 285–293.

MCDONNELL, J. A. M. (1978). Microparticle studies by space instrumentation. In *Cosmic Dust* (J. A. M. McDonnell, Ed.), pp. 337–426. Wiley, Chichester.

MCDONOUGH, T. R. (1975). Effects of stellar spin and diameter on Poynting–Robertson drag. Presented to N.Y. Astronomical Corp. meeting, April.

MCDONOUGH, T. R., AND BRICE, N. M. (1973). A Saturnian gas ring and the recycling of Titan's atmosphere. *Icarus* **20**, 136–145.

MENDIS, D. A., AND AXFORD, W. I. (1974). Satellites and magnetospheres of the outer planets. *Ann. Rev. Earth Planet. Sci.* **2**, 419–474.

MILLMAN, P. M. (1971). The meteoritic hazard of interplanetary travel. *Amer. Sci.* **59**, 700–705.

MILLMAN, P. M. (1976). Meteors and interplanetary dust. In *Interplanetary Dust and Zodiacal Light* (H. Elsässer and H. Fechtig, Eds.), pp. 359–372. Springer-Verlag, Berlin.

MISCONI, N. Y., AND WEINBERG, J. L. (1978). Is Venus concentrating interplanetary dust toward its orbital plane? *Science* **200**, 1484–1485.

MORAVEC, T. J., RIFE, J. C., AND DEXTER, R. N. (1976). Optical constants of nickel, iron and nickel-iron alloys in the vacuum ultraviolet. *Phys. Rev. B* **13**, 3297–3306.

MORRISON, D. (1977). Radiometry of satellites and of the rings of Saturn. In *Planetary Satellites* (J. A. Burns, Ed.), pp. 269–301. Univ. of Arizona Press, Tucson.

MORRISON, D., AND BURNS, J. A. (1976). The Jovian satellites, In *Jupiter* (T. Gehrels, Ed.), pp. 991–1034. Univ. of Arizona Press, Tucson.

MORRISON, D. A., AND ZINNER, E. (1975). Studies of solar flares and impact craters in partially protected crystals. *Proc. 6th Lunar Sci. Conf.* **3**, 3373–3390.

MORRISON, D. A., AND ZINNER, E. (1977). 12054 and 76215: New measurements of interplanetary dust and solar flare fluxes. *Proc. 8th Lunar Sci. Conf.,* 841–863.

MUKAI, T., AND MUKAI, S. (1973). Temperature and motion of grains in interplanetary space. *Publ. Astron. Soc. Japan* **25**, 481–488.

MUKAI, T., YAMAMOTO, T., HASEGAWA, H., FUJIWARA, A., AND KOIKE, C. (1974). On the circumsolar grain materials. *Publ. Astron. Soc. Japan* **26**, 445–458.

MULLAN, D. J. (1977). Dust from the Sun? *Astron. Astrophys.* **61**, 369–375.

MUSEN, P. (1960). The influence of the solar radiation pressure on the motion of an artificial satellite. *J. Geophys. Res.* **65**, 1391–1396.

NAGEL, K., NEUKUM, G., FECHTIG, H., AND GENTNER, W. (1976). Density and composition of interplanetary dust particles. *Earth Planet. Sci. Lett.* **30**, 234–240.

NEIMAN, V. B., ROMANOV, E. M., AND CHERNOV, V. M. (1965). Ivan Osipovich Yarkovsky. *Zeml'ya Vselennaya* No. 4, 63–64.

NEY, E. P. (1977). Star dust. *Science* **195**, 541–546.

ÖPIK, E. J. (1951). Collision probabilities with the planets and the distribution of interplanetary matter. *Proc. Roy. Ir. Acad.* **54**, 165–199.

ÖPIK, E. J. (1956). Interplanetary dust and terrestrial accretion of meteoric matter. *Ir. Astron. J.* **4**, 84–135.

OVER, J. (1958). On the vaporization of solid particles near the Sun. *Kon. Ned. Akad. Westensch. Proc. Ser. B* **61**, 74–85.

PADDACK, S. J. (1969). Rotational bursting of small celestial bodies: Effects of radiation pressure. *J. Geophys. Res.* **74**, 4379–4381.

PADDACK, S. J., AND RHEE, J. W. (1976). Rotational bursting of interplanetary dust particles. In *Interplanetary Dust and Zodiacal Light* (H. Elsässer and H. Fechtig, Eds.), pp. 453–457. Springer-Verlag, Berlin.

PARKER, E. N. (1964). The perturbation of interplanetary dust grains by the solar wind. *Astrophys. J.* **139**, 951–958.

PARKIN, D. W., SULLIVAN, R. A. L., AND ANDREWS, F. N. (1977). Cosmic spherules as rounded bodies in space. *Nature* **266**, 515–517.

PARTHASARATHY, R. (1979). Cometary origin of interplanetary submicron dust. *Astron. J.* **84**, 143–147.

PEALE, S. J. (1966). Dust belt of the Earth. *J. Geophys. Res.* **71**, 911–933; see also *J. Geophys. Res.* **72**, 1124–1127.

PETERSON, C. A. (1966). Use of thermal reradiative effects in spacecraft attitude control. Report CSR

T-66-3 (also M.S. thesis). Massachusetts Institute of Technology.

PETERSON, C. (1976). A source mechanism for meteorites controlled by the Yarkovsky effect. *Icarus* **29**, 91–111.

POLLACK, J. B., TOON, O. B., AND KHARE, B. N. (1973). Optical properties of some terrestrial rocks and glasses. *Icarus* **19**, 372–389.

POLLACK, J. B., WITTEBORN, F. C., ERICKSON, E. E., STRECKER, D. W., BALDWIN, B. J., AND BUNCH, T. E. (1978). Near infrared spectra of the Galilean satellites: Observations and compositional implications. *Icarus*, **36**, 271–303.

RADZIEVSKII, V. V. (1952). On the influence of an anisotropic re-emission of solar radiation on the orbital motion of asteroids and meteorites. *Astron. Zh.* **29**, 162–170. U.S. Dept. of Commerce translation 62-10653.

RADZIEVSKII, V. V. (1954). A mechanism of the disintegration of asteroids and meteorites. *Dokl. Akad. Nauk SSSR* **97**, 49–52.

RADZIEVSKII, V. V. (1967). Gravitational capture of cosmic dust by the Sun and planets and evolution of the circumterrestrial cloud. *Sov. Astron.-AJ* **11**, 128–136.

RADZIEVSKII, V. V., AND ARTEM'EV, A. V. (1962). The influence of solar radiation pressure on the motion of artificial earth satellites. *Sov. Astron.-AJ* **5**, 758–759.

RAJAN, R. S., AND WEIDENSCHILLING, S. J. (1977). Dynamics of small particles in the solar system. *Bull. Amer. Astro. Soc.* **9**, 519.

RHEE, J. W. (1976). Radial distribution of meteoric particles in interplanetary space. In *Interplanetary Dust and Zodiacal Light* (H. Elsässer and H. Fechtig, Eds.), pp. 448–452. Springer-Verlag, Berlin.

ROBERTSON, H. P. (1937). Dynamical effects of radiation in the solar system. *Mon. Not. Roy. Astron. Soc.* **97**, 423–438.

SCHWEHM, G. (1976). Radiation pressure on interplanetary dust particles. In *Interplanetary Dust and Zodiacal Light* (H. Elsässer and H. Fechtig, Eds.), pp. 459–463. Springer-Verlag, Berlin.

SCHWEHM, G., AND RHODE, M. (1977). Dynamical effects on circumsolar dust grains. *J. Geophys.* **42**, 727–735.

SEHNAL, L. (1969). Radiation pressure effects in the motion of artificial satellites. In *Dynamics of Satellites* (B. Morando, Ed.), pp. 262–272. Springer-Verlag, Berlin.

SEKANINA, Z. (1976). Modeling of the orbital evolution of vaporizing dust particles near the Sun. In *Interplanetary Dust and Zodiacal Light* (H. Elsässer and H. Fechtig, Eds.), pp. 434–436. Springer-Verlag, Berlin.

SEKANINA, A., AND SCHUSTER, H. E. (1978a). Meteoroids from periodic Comet d'Arrest. *Astron. Astrophys.* **65**, 29–35.

SEKANINA, Z., AND SCHUSTER, H. E. (1978b). Dust from periodic Comet Encke: Large grains in short supply. *Astron. Astrophys.* **68**, 429–435.

SHAPIRO, I. I. (1963). The prediction of satellite orbits. In *The Dynamics of Satellites* (M. Roy, Ed.), pp. 257–312. Academic Press, New York.

SHAPIRO, I. I., AND JONES, H. M. (1961). Effects of the Earth's magnetic field on the orbit of a charged satellite. *J. Geophys. Res.* **66**, 4123–4127.

SHAPIRO, I. I., LAUTMAN, D. A., AND COLOMBO, G. (1966). Earth's dust belt: Fact or fiction? 1. Forces perturbing dust particle motion. *J. Geophys. Res.* **71**, 5694–5704.

SINGER, S. F., AND BANDERMANN, L. W. (1967). Nature and origin of zodiacal dust. In *The Zodiacal Light and the Interplanetary Medium* (J. L. Weinberg, Ed.), pp. 379–397, NASA SP-150.

SLABINSKI, V. S. (1977). Solar radiation torque on meteoroids: Complications for the Yarkovsky effect from spin axis precession. *Bull. Amer. Astro. Soc.* **9**, 438.

SOBERMAN, R. K. (1971). The terrestrial influx of small meteoric particles. *Rev. Geophys. Space Phys.* **9**, 239–258.

SOTER, S. (1971). The dust belts of Mars. Cornell University CRSR Rept. No. 462. Also in Ph.D. thesis, Cornell University.

SOTER, S. (1974). Brightness asymmetry of Iapetus. Presented at IAU Colloquium No. 28, Cornell University, August 1974.

SOTER, S., BURNS, J. A., AND LAMY, P. L. (1977). Radiation pressure and Poynting–Robertson drag for small spherical particles. In *Comets, Asteroids and Meteorites* (A. Delsemme, Ed.), pp. 121–125. Univ. of Toledo Press, Toledo, Ohio.

STANDEFORD, L. (1968). *The Dynamics of Charged Interplanetary Grains*. Ph.D. thesis, University of Illinois.

STEYER, T. R. (1974). *Infrared Optical Properties of Some Solids of Possible Interest in Astronomy and Atmospheric Physics*. Ph.D. thesis, Univ. of Arizona.

STEYER, T. R., DAY, K. L., AND HUFFMAN, D. R. (1974). Infrared absorption by small amorphous quartz spheres. *Appl. Opt.* **13**, 1586–1590.

TAFT, E. A., AND PHILLIPPS, H. R. (1965). Optical properties of graphite. *Phys. Rev. A* **138**, 197–202.

VAN DE HULST, H. C. (1957). *Light Scattering by Small Particles*. Wiley, New York.

VANYSEK, V. (1976). Dust in comets and interplanetary matter. In *Interplanetary Dust and Zodiacal Light* (H. Elsässer and H. Fechtig, Eds.), pp. 299–313. Springer-Verlag, Berlin.

VAARANIEMI, P. (1973). The short-periodic perturbations in Saturn's rings. Rpt. 14, Aarne Karjalainen Obs., Oulu, Finland. NASA N73-19854.

VEDDER, J. F., AND MANDEVILLE, J.-C. (1974). Mi-

crocraters formed in glass by projectiles of various densities. *J. Geophys. Res.* **79**, 3247–3256.

VERNAZZA, J. E., AVRETT, E. H., AND LOESSER, R. (1976). Structure of the solar chromosphere. II. The underlying photosphere and temperature-minimum region. *Astrophys. J. Suppl.* **30**, 1–60.

WEIDENSCHILLING, S. J. (1978). The distribution of orbits of cosmic dust particles detected by Pioneers 8 and 9. *Geophys. Res. Lett.* **5**, 606–608.

WEINBERG, J. L., ED. (1967). *The Zodiacal Light and the Interplanetary Medium.* NASA SP-150.

WEINBERG, J. L. (1976). Space observations of the zodiacal light. In *Interplanetary Dust and Zodiacal Light* (H. Elsässer and H. Fechtig, Eds.), pp. 3–18, Springer-Verlag, Berlin.

WEINBERG, J. L., AND SPARROW, J. G. (1978). Zodiacal light as an indicator of interplanetary dust. In *Cosmic Dust* (J. A. M. McDonnell, Ed.), pp. 75–122. Wiley, Chichester.

WETHERILL, G. W. (1974). Solar system sources of meteorites and large meteroids. *Ann. Rev. Earth Planet. Sci.* **2**, 303–331.

WHIPPLE, F. L. (1955). A comet model. III. The zodiacal light. *Astrophys. J.* **121**, 750–770.

WHIPPLE, F. L. (1967). On maintaining the meteoritic complex. In *The Zodiacal Light and the Interplanetary Medium* (J. Weinberg, Ed.), pp. 409–426, NASA SP-150.

WHIPPLE, F. L. (1976). Sources of interplanetary dust. In *Interplanetary Dust and Zodiacal Light* (H. Elsässer and H. Fechtig, Eds.), pp. 403–415. Springer-Verlag, Berlin.

WHIPPLE, F. L. (1978). Comets. In *Cosmic Dust* (J. A. M. McDonnell, Ed.), pp. 1–73. Wiley, Chichester.

WHIPPLE, F. L., AND HUEBNER, W. F. (1976). Physical processes in comets. *Ann. Rev. Astron. Astrophys.* **14**, 143–172.

WICKRAMASINGHE, N. C. (1972). On the injection of grains into interstellar clouds. *Mon. Not. Roy. Astron. Soc.* **159**, 269–287.

WOLSTENCROFT, R. D., AND ROSE, L. J. (1967). Observations of the zodiacal light from a sounding rocket. *Astrophys. J.* **147**, 271–292.

WYATT, S. P., AND WHIPPLE, F. L. (1950). The Poynting–Robertson effect on meteor orbits. *Astrophys. J.* **111**, 134–141.

ZERULL, R. (1976). Scattering functions of dielectric and absorbing irregular particles. In *Interplanetary Dust and Zodiacal Light* (H. Elsässer and H. Fechtig, Eds.), pp. 130–134. Springer-Verlag, Berlin.

ZERULL, R. H., GIESE, R. H., AND WEISS, K. (1977a). Scattering functions of non-spherical dielectric and absorbing particles vs. Mie theory. *Appl. Opt.* **16**, 777–778.

ZERULL, R. H., GIESE, R. H., AND WEISS, K. (1977b). Interpretation of zodiacal light brightness and polarization by scattering properties of irregular and fluffy micrometeroids. Presentation to COSPAR meeting in Tel Aviv, Israel.

ZOOK, H. A. (1975). Hyperbolic cosmic dust: Its origin and its astrophysical significance. *Planet. Space Sci.* **23**, 1391–1397.

ZOOK, H. A., AND BERG, O. E. (1975). A source for hyperbolic cosmic dust particles. *Planet. Space Sci.* **23**, 183–203.